Tampereen yliopisto

Petri Seppä

UTILIZATION OF WATER FLOW MEASUREMENT IN A RIVER SYSTEM

Faculty of Engineering and Natural Sciences
Master of Science Thesis
June 2019

ABSTRACT

Petri Seppä: Utilization of water flow measurement in a river system
Master of Science Thesis
Tampere University
Master's Degree Programme in Electrical Engineering
June 2019

Hydropower is significant form of electricity production in the Nordics. Over half of the produced electricity in the Nordics is hydropower. Hydropower is a renewable source of low-cost electricity with great flexibility. The production of hydropower on a large scale is dependent on the present hydrological balance. The availability of hydropower is the one of the main drivers of the electricity price in the Nordics. The hydropower producers aim at optimized production by allocating the production on different markets and periods when the electricity is expensive. Flexible operation on different markets causes variation in the discharges of hydropower units. This creates a demand for models which are used to forecast the water levels. Modeling the dynamics of water requires understanding of the phenomena in a river system.

This thesis studies the utilization of water flow measurement in a river system with hydro assets. Two water flow meters were installed in a river system located in Finland. The aim of this thesis is to develop a water level forecasting for the river system, especially a specific section of it. The river section examined in this thesis has proven to be the most difficult to model accurately.

Data acquired from the water flow meters allowed to model the relationship between the height difference of the water levels and the water flow of the river. A new forecasting model was created where the river section is divided into three separate reservoirs. The inflows and outflows of the reservoirs are calculated using the regression lines.

The new forecasting tool should be considered as a concept that could be developed further, because the forecast created using the new model does not systemically outperform the old tools. The results in modeling the river section as multiple reservoir looks promising.

Based on the results presented in this thesis, future research should include the usage of temporally water level measurement. This should provide more accurate data enabling the accuracy to be developed more.

Keywords: Water flow measurement, hydropower, forecast, modeling, water system development

TIIVISTELMÄ

Petri Seppä: Virtaamamittauksen hyödyntäminen jokivesivoiman tuotannossa
Diplomityö
Tampereen yliopisto
Sähkötekniikan diplomi-insinöörin tutkinto-ohjelma
Kesäkuu 2019

Vesivoima on merkittävä sähkön tuotantomuoto pohjoismaissa. Yli puolet pohjoismaissa tuotetusta sähköstä on vesivoimaa. Vesivoima on kustannustehokas uusiutuvan energian tuotantomuoto, jolla on suuri joustavuus. Vesivoiman tuotanto riippuu suuressa mittakaavassa vallitsevasta vesitilanteesta. Vesivoiman varastointitilanne ja kapasiteetin joustavuus on yksi suurimpia sähkön hintaan vaikuttavia tekijöitä pohjoismaissa. Vesivoiman tuottajat pyrkivät optimoimaan tuotantoaan allokoimalla sitä eri markkinoille ja ajanjaksoille, jolloin sähkön tuottaminen on kannattavinta.

Joustava toimiminen eri markkinoilla aiheuttaa vesivoimaloiden virtaamien vaihteluita. Tästä syntyy tarve malleille, joita käytetään vesipintojen ennustamiseen. Veden dynamiikan mallintaminen jokisysteemissä vaatii systeemin ilmiöiden ymmärrystä.

Työssä tutkitaan virtaamamittareiden hyödyntämisessä jokivesivoiman tuotannossa. Kaksi virtaamamittaria on asennettu jokeen, joka sijaitsee Suomessa. Työn tavoitteena on kehittää vesipintojen ennustamista jokisysteemissä, erityisesti yhdessä tietyssä jokiosuudessa. Työssä tutkittu jokiosuus on osoittautunut aiemmissa töissä haasteelliseksi mallintaa tarkasti.

Virtaamamittareista saadun datan avulla löydettiin sovitteet korrelaatiolle joen virtaaman ja pintamittausten korkeuserojen välillä. Uusi ennustemalli luotiin jakamalla jokiuoma kolmeen erilliseen altaaseen. Tulo- ja lähtövirtaamat näistä altaista saadaan laskettua sovitteiden avulla.

Työssä luotua ennustemallia tulee tarkastella menetelmänä, jonka pohjalta kehitystä voidaan jatkaa. Ennustemallin tarkkuus ei nykyisellä tarkkuudella ole systemaattisesti parempi kuin vanhoilla malleilla. Tulokset jokiosuuden mallintamiselta useassa altaassa vaikuttavat kuitenkin lupaavilta.

Työssä saatujen tulosten perusteella esitetyn jatkotutkimuksen on suositeltava pitää sisällään väliaikaisen pintamittauksen hyödyntämistä. Tämän mittauksen tuottamalla tarkemmalla datalla mallin tarkkuutta on mahdollista parantaa.

Avainsanat: Virtaamamittaus, vesivoima, ennuste, mallinnus, vesistön kehitys

PREFACE

This thesis was written for UPM Energy and for the department of Electrical Engineering of Tamper University.

I would like to thank UPM Energy for providing me this challenging opportunity to work with interesting topic. Also, I would like to thank my instructor M.Sc (Tech) Matti Vuorinen for all the ideas and guidance during this project. Furthermore, I would like to thank Professor Pertti Järventausta for all the advices for completing this thesis. I would also like to than M.Sc (Tech) Lari Pelkola for all the help during this project. It has been a joy working with you.

I am also thankful to my family and Sini for all the support during my studies.

Tampere, June 20, 2019

Petri Seppä

CONTENTS

ABBREVIATIONS

ADCP	Acoustic Doppler Current Profiler
aFRR	Automatic Frequency Restoration Reserve
FCR-D	Frequency Containment Reserve for Disturbances
FCR-N	Frequency Containment Reserve for Normal Operation
Hour unit (HU)	Hydropower discharge hour unit, $1\ HU = 3600\ m^3$
mFRR	Manual Frequency Restoration Reserve
MAE	Mean Absolute Error
TSO	Transmission System Operator
RoR	Run-of-River type of hydropower
SCF	Storing Capacity Factor

1. INTRODUCTION

This thesis studies the utilization of two water flow measurements in a specific hydropower system. The thesis includes an introduction of the Nordic electricity market and a theoretical analysis of the production and planning of hydropower. The physical electricity market can be divided into two components, the day-ahead market and the intraday-market. The focus on the utilization of the water flow measurements is on the physical markets, more precisely on the intraday operation and the production planning

1.1 Background

Hydropower is the most important and traditional form of renewable energy for electricity generation because of its good abilities to balance the power system (Singh and Singal, 2017). With an ordinary precipitation of water and snow, hydropower production covers half of the electricity demand in the Nordics (Nordic Energy Regulators, 2014). In Finland, 23% of the electricity produced was hydropower in 2017. A normal level of hydropower production is 13 TWh in Finland (Energiateollisuus, 2019a). Because of the significant portion of the electricity produced, hydropower has a substantial effect on the hourly electricity price in the Nordics (Nordic Energy Regulators, 2014).

The Nordic electricity wholesale market for the following day is called Elspot and is offered by Nord Pool. Bids for the following day must be delivered not later than 12:00 CET. A buyer decides the needed amount of electricity in order to meet the demand for the following day. The buyer also decides how much it is willing to pay for the electricity hourly. A seller decides how much it is willing to sell and on what price. For example, the owner of the hydropower plant is a seller. (Nord Pool, 2019b). The market price for electricity is different hour by hour. Hourly differences originate on the changing balance of the electricity production and consumption (Nord Pool, 2019e). Therefore, hydropower producers need to plan the production hourly to maximize the profit of the electricity produced.

Hydropower producers widely use optimization tools to schedule the production. Optimization tools require advanced forecasts of the inflow and price in order to find the optimal solution for the electricity production. The goal is to time the release of the water from the upper reservoir in the river system to maximize the expected value from the production. Challenges arise in situations where the inflow forecasts are inaccurate or the timing of the release of the water from the upper reservoir is difficult. Deviations between the forecasted and realized inflow can cause situations where the production sold to the day-ahead market cannot be realized. The imbalance of

the production can be traded in the intraday-market to minimize the cost (Scharff *et al.*, 2014; Ødegård, Eidsvik and Fleten, 2019).

1.2 Research Objectives

This thesis studies the utilization of the water flow measurements in a river system located in the Nordic area. The main objective of the research is to study how to take advantage of the two water flow meters installed in the river system with hydro assets. The hydropower plants in the river are operated by a producer that uses a forecasting model to anticipate the near future water levels and discharges. The previous forecasting model has been created for the planning of the production on the physical market. The tool simulates the water levels using planned discharges and forecasted runoffs for all the hydropower plants in the river system for 72 hours ahead with the forecasting resolution of one hour. The tool is used both in the day-ahead and intraday planning. This thesis aims at improving the whole forecasting horizon, but particularly the next 12 hours ahead. The next 12 hours is the most essential time horizon in the intraday operation and planning.

The research questions are presented below:

1. How can the two water flow measurements improve the operation and planning of the river system?
2. Can the current forecasting models be improved by using additional data available?
3. For how long does the operator have to act when a relevant change in the runoff is noticed?

1.3 Structure

This thesis consists of six chapters starting with an introduction chapter and finishing with a conclusion chapter. The beginning of the thesis is a theoretical foundation of the topics examined in this study. The empirical parts of the thesis start in the chapter 4. The thesis structure is presented as follows.

The second chapter introduces the Nordic electricity market. The financial market is handled briefly in this chapter. Analysis of the physical markets consists of the day-ahead market and intraday market. This part presents the characteristics of the physical market including an analysis of the Nordic electricity market area, transmission lines and price areas. It continues with the basics behind price formation in the day-ahead market and fundament features of the intraday market. Finally, the chapter 2 presents the introduction of power balance market and the frequency containment reserves.

The third chapter focuses on hydropower. The chapter begins with an analysis of hydropower including the explanation of hydropower plants and electricity generation. The chapter continues

with an examination of run-of-river hydropower and explanation of water dynamics in a river system. At the end of the chapter is an inspection of hydropower production planning including the main principles regarding the planning and operation process of hydropower.

The fourth chapter analyses the river system studied in this thesis. The reservoirs and hydropower units are presented first. The constraints regarding the operation and planning of the hydropower units in the river system are presented after the analysis of the river system. Chapter 4 also focuses on the uncertainties in the planning and operation of the river system.

The new model created in this thesis is presented in the fifth chapter. The new model is used to forecast the water levels in the river system. Chapter illustrates the main differences in the structure of the model when compared to the previously used forecasting model. The strengths and areas that require more development are analyzed and presented. The chapter also illustrates the performance of the model with two forecasts which are calculated using the new model.

The final chapter is the conclusion chapter. It analyses the results of this thesis and introduces proposals to improve the operation and planning of the river system.

2. THE NORDIC ELECTRICITY MARKET

In 1996 the joint Norwegian-Swedish power exchange, Nord Pool, was established. Finland joined the Nordic electricity market in 1998. Later, the market expanded to Denmark, Lithuania, Latvia, Estonia and the United Kingdom (Nord Pool, 2019a). The power transmission between countries has increased over the years (Nord Pool, 2019c). Politicians and other stakeholders agree that the current deregulated model of the electricity exchange is serving the society well (Nord Pool, 2019c).

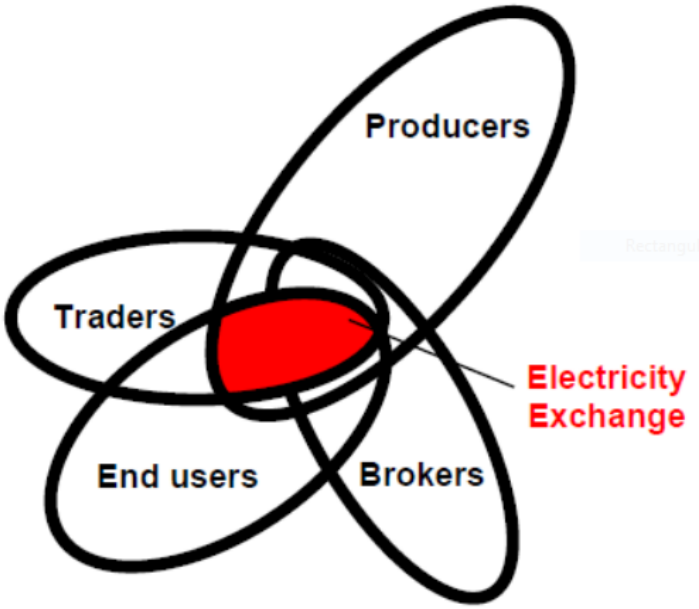

Figure 1. *The commercial participants of the Nordic electricity market are traders, end users, brokers and producers. The intersection of the sets is marked as red and it presents the varying backgrounds of the actors in the electricity market. The figure illustrates that all actors in the energy sector does not participate in the electricity exchange. (Nord Pool, 2018)*

As seen in Figure 1, the participants in the Nordic electricity market can be divided into four categories. The producers are companies that own the production plants. The traders own the electricity during the trading process. For example, a trader can purchase electricity from a producer and sell it to a retailer or another trader. The role of the broker is similar to the trader, but the broker does not own the electricity. The end users are the participants that consume the produced electricity. (Nord Pool, 2018)

Next, the characteristics of the deregulated electricity market in the Nordics are introduced. Section 2.1 demonstrates the price areas in the Nordic and section 2.2. focuses on different electricity markets.

2.1 Price areas

An integrated power market enables the transmission of the power between the countries in the Nordics. This leads to an efficient use of the electricity available and more secure supply of the electricity. Transmission of electricity between countries arises in situations where demand and supply in a certain area are not balanced. In these situations, power flow from the low price area to the high price area. This principle can be seen as maximization of social welfare because commodity ought to move towards the high price where the demand is the highest. Area prices may vary between areas due to bottlenecks in transmission capacity. (Nord Pool, 2019a)

The price areas are being formed by the transmission lines between countries and additionally by the local transmission system operator (TSO) decisions to divide the country into multiple bidding areas (Nord Pool, 2019a). The TSOs own the national transmission system and are responsible for the secure supply of electricity in their own area (Flatabo *et al.*, 2003). Finland and the Baltics form their own price areas, whereas Norway, Sweden and Denmark are divided into a few price areas each (Nord Pool, 2019d). Figure 2 below presents the Nordic electricity market price areas and area prices in a specific hour in January 2019.

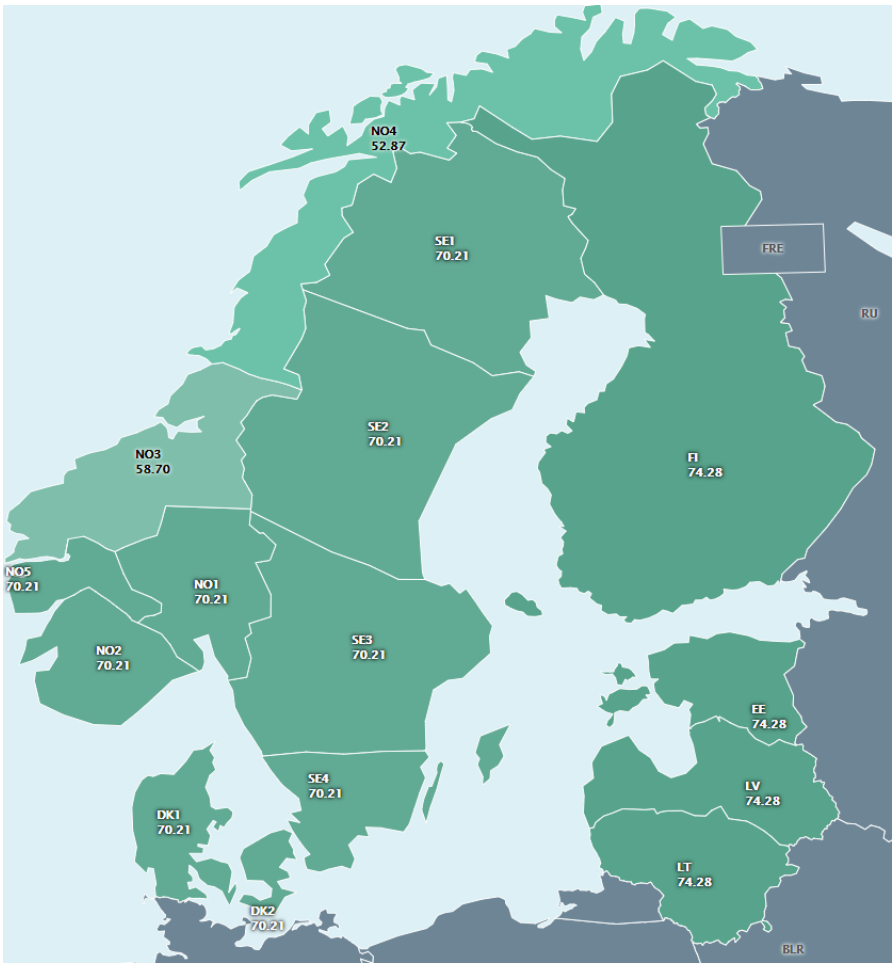

Figure 2. *The Nordic electricity market price areas and area prices (€/MWh) on hour 17, 22nd of January 2019 (Nord Pool, 2019d).*

Figure 2 above presents a situation, where the transmission capacity between Sweden and Finland is at its limit. The area price in Finland is higher than in Sweden, but the limitations in the transmission capacity prevent the import of the electricity to Finland. Thus, the lack of electricity needs to be covered with a more expensive form of production in Finland or the Baltics.

Figure 3 below illustrates the hourly electricity area price on week 3 in Finland (FI) and Sweden area 1 (SE1).

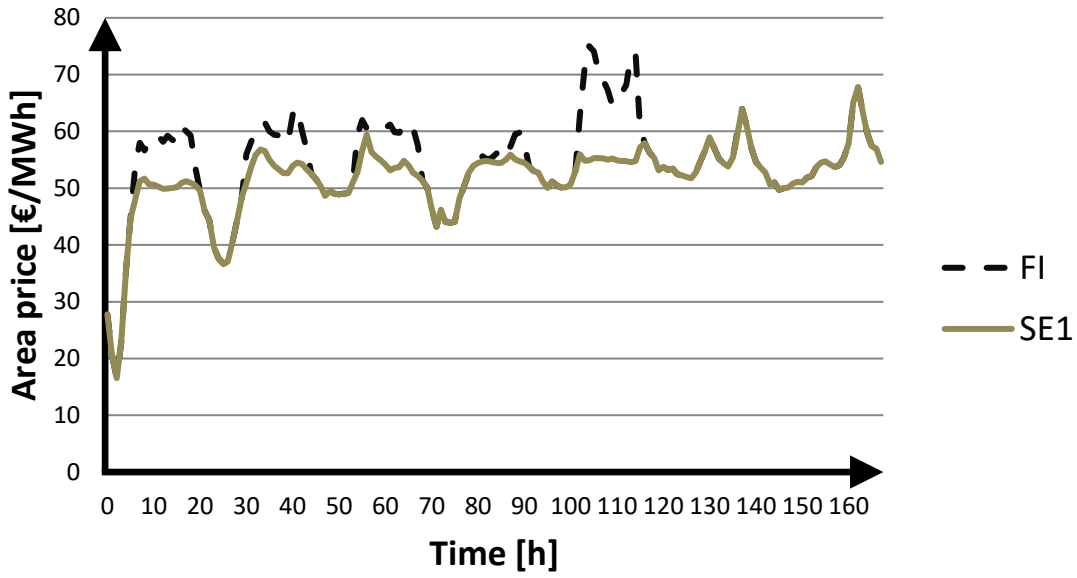

Figure 3. *Hourly electricity area price in FI and SE1 for a week 3 in January 2019. The first five days where the prices differ are weekdays and the last two are weekend. The area price is higher in Finland on weekdays. The figure demonstrates the typical variation between prices on day and night. Usually, the electricity price is higher during the day than night.*

The demand for electricity is typically higher during the day hours of weekdays, which explains the price difference. The figure also shows that the area prices are identical on the weekend. In that case, the transmission lines from northern Sweden to Finland are not at their full capacity and areas merge resulting in the same price of the electricity.

The integrity of the price areas is presented in Figure 4 below.

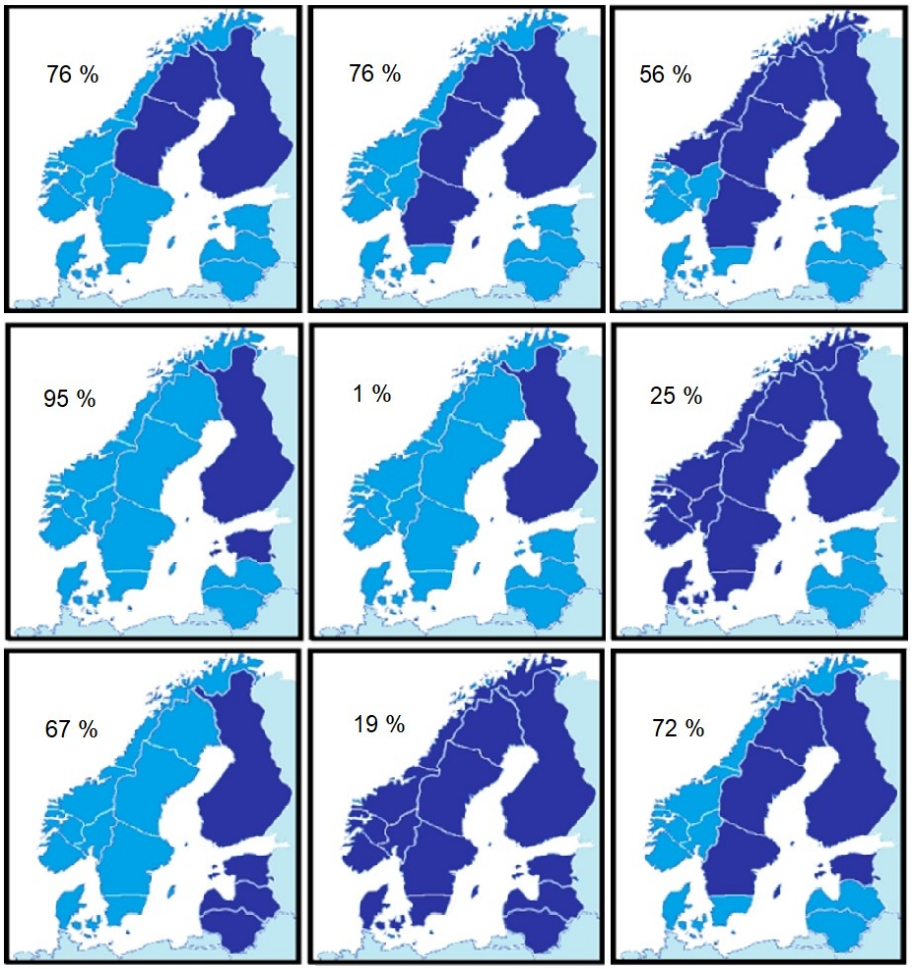

Figure 4. *The integrity of price areas in 2018 (Fingrid, 2019b). The dark blue color indicates bidding areas which have shared a common day-ahead electricity price. The percentage in the scenarios state the number of hours these areas have shared a common price in 2018.*

As the figure presents, Finland is rarely a separated price area. Only 1 % of the hours in 2018 the transmission capacity between Finland and the bidding zones SE1, SE3, NO4 and EE were at the full capacity. (Fingrid, 2019b)

2.2 Market Structure

This section presents the physical and financial markets. The structure of the Nordic power market is summarized in Table 1. Nasdaq OMX Commodities offer the financial contracts market for electricity. The time horizon for the financial contracts can vary from days to six years. The physical electricity market is offered by Nord Pool. The physical electricity exchange provides the market for the current and following day. The power balance market is offered by the TSOs. This market ensures that the demand and supply are in balance real time.

Table 1. *The structure of the Nordic power market. Adapted from Kinnunen (2013).*

	Physical contracts				Financial contracts
Provider	TSOs		Nord Pool		Nasdaq OMX Commodities
Market	Reserves	Regulating market	Intraday market	Day-ahead market	Financial market
Time scale	Continuous from seconds	15-60 minutes	Hours	Hours next day	daily weekly monthly quarterly annually

2.2.1 Financial Market

The deregulation of the Nordic power market has caused an increased volatility in the day-ahead electricity prices (Kinnunen, 2013). Nasdaq OMX Commodities provide a marketplace where market members can trade financial contracts used generally for the price hedging, risk management of the trade in electric power and other trading purposes. The financial market contains only cash-settled contracts with no physical delivery of the electricity. (Nasdaq Commodities, 2019)

The contract types traded in the financial market comprise power derivates such as futures, DS futures, options, and EPAD contracts. The financial contracts have a time horizon up to ten years, covering annual, quarterly, monthly, weekly and daily contracts. The cash settlement of the contracts can take place throughout the trading or delivery period. The system price of Nord Pool physical exchange is used as a reference price for the financial market. The financial market bypasses the physical constrains of the power grid, such as the grid congestion and access to capacity. (Nasdaq Commodities, 2019; Nord Pool, 2019f)

A future contract is an agreement to sell or buy a predetermined amount of electricity for a fixed price at a certain time in the future. The difference between futures and DS futures are that a cash settlement is done on the daily basis for futures and at the end of the due date of the contract for the DS futures. An option is an opportunity to buy or sell an underlying contract at a fixed price at a certain date in the future. Electricity price area differentials (EPADs) are contracts used for the hedging against the price differences between the area price and system price. (Nasdaq Commodities, 2019)

Financial contracts are being used for the signaling the future electricity prices. These signals support the decision making regarding the future development of the supply and demand of the

electricity. The physical market cannot provide long term price signals due to the short trading horizon. (Kinnunen, 2013)

2.2.2 Physical Market

The physical market for electricity in the Nordics and Baltics if offered by Nord Pool. The delivery of the electricity is offered hourly every day. The day-ahead market is called Elspot and it covers 98 % of the traded electricity in the Nordics and Baltics. Elspot is a closed auction-based market where market participants specify the volume in MW, which they are willing to buy or sell at pre-determined price €/MWh for each hour on the following day. The market participants must place their orders by 12:00 (CET). These hourly orders are aggregated into supply and demand curves demonstrated in Figure 5 below.

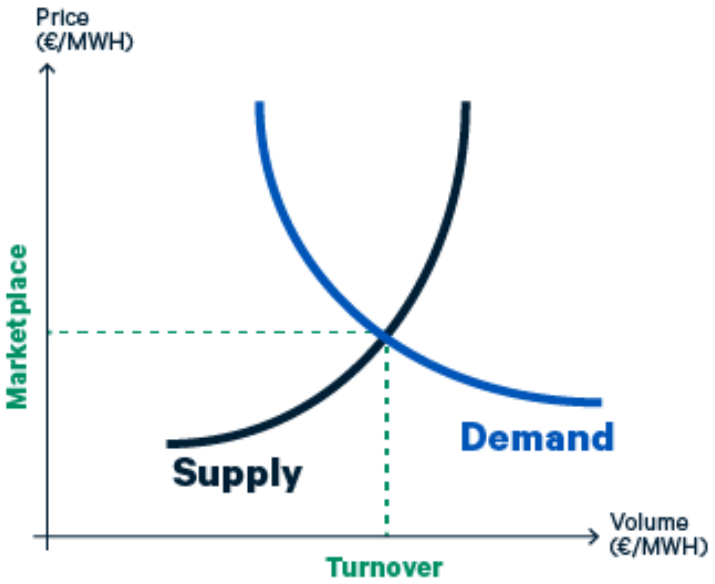

Figure 5. *Aggregated supply and demand curves in the day-ahead market. The hourly price for the electricity is set to the point where the supply and demand curves cross. (Nord Pool, 2019b)*

If there are no constrains in the transmission capacity between the bidding areas, hourly prices are congruent in all areas. On the other hand, if the transmission capacity between the bidding areas gets constrained, the electricity price is raised to reduce the demand and increase production in the areas affected. (Nord Pool, 2019b)

As mentioned in Section 2.2.1, the system price typically differs from area prices. The system price is based on all biding areas demand and supply orders disregarding available transmission capacities between the bidding areas. The financial contracts use the Nordic system price as a reference price. (Nord Pool, 2019a)

The day-ahead prices are made public at around 12:30-12:45 (CET). Then the producers will know how much electricity they are committed to deliver for every hour in the following day (Alnæs

et al., 2015). The initial production plan offered to the day-ahead market is typically found by an optimization tool. Unpredictable events, such as a considerable change in the forecasted inflow or technical malfunctions, causes deviations from the initial production plan. (Skjelbred and Kong, 2018)

In these cases, the producer is not capable or willing to deliver the amount of electricity sold to the day-ahead market. Adjustment trades are needed to comply with the committed volume. For this purpose, the market operator offers the intraday market. (Alnæs *et al.*, 2015)

Nord Pool offers intraday market called Elbas. It is a supplementary market allowing the trading closer to the delivery hour. In 2017, the traded volume in the intraday market was 6.7 TWh which, equals to 1.7% of the total volume traded in the Nordics (Nord Pool, 2017). The intraday market allows trading continuously around the clock, up to an hour prior to the delivery. Trading closer to the delivery hour offers producers and consumers better insight into their imbalance volumes. This allows to the market participants an opportunity to minimize their imbalance costs. One of the benefits of the intraday trading is to hedge against the imbalance costs. Market participants are exposed to imbalance costs when supplying more or less electricity than planned. The imbalance price may deviate significantly from the day-ahead prices. (Scharff and Amelin, 2015). Pogosan and Windberg (2013) conducted a survey among the Swedish balance responsible companies which stated that the reduction of imbalance costs is the main motivation for intraday trading.

Continuous trading in the intraday market means that prices are set based on a first-come, first-served principle, where the best prices are traded first, i.e. the buying bid with the highest offer price and the selling offer with the lowest ask price are met first. The continuous trading also causes significant variation in the prices because traders are settled within a time period whenever a market participant accepts an offer from another participant. (Scharff and Amelin, 2015)

2.2.3 Power Balance Market

The consumption and production of electricity must always be equal. The possible imbalance between the production and consumption affects the frequency of the power grid. Market operators plan their production and consumption in advance and trade the excess or deficit in the Elspot or Elbas markets. In practice, deviations between the production and consumption occurs during each hour and the frequency of the grid varies from its nominal value 50 Hz. The frequency of the grid can vary between 49,9 and 50,1 Hz in a nominal situation. Less production than consumption causes the frequency to decrease from the nominal 50 Hz. On the contrary, the frequency exceeds 50 Hz when production is greater than consumption. TSOs procures different kinds of reserves from the power balance market to balance these deviations. Reserves are production plants or consumption units which either decrease or increase their electric power. (Entsoe, 2017; Fingrid, 2019c)

The frequency control process used in Finland to continuously balance momentary variations between production and consumption is presented below in Figure 6.

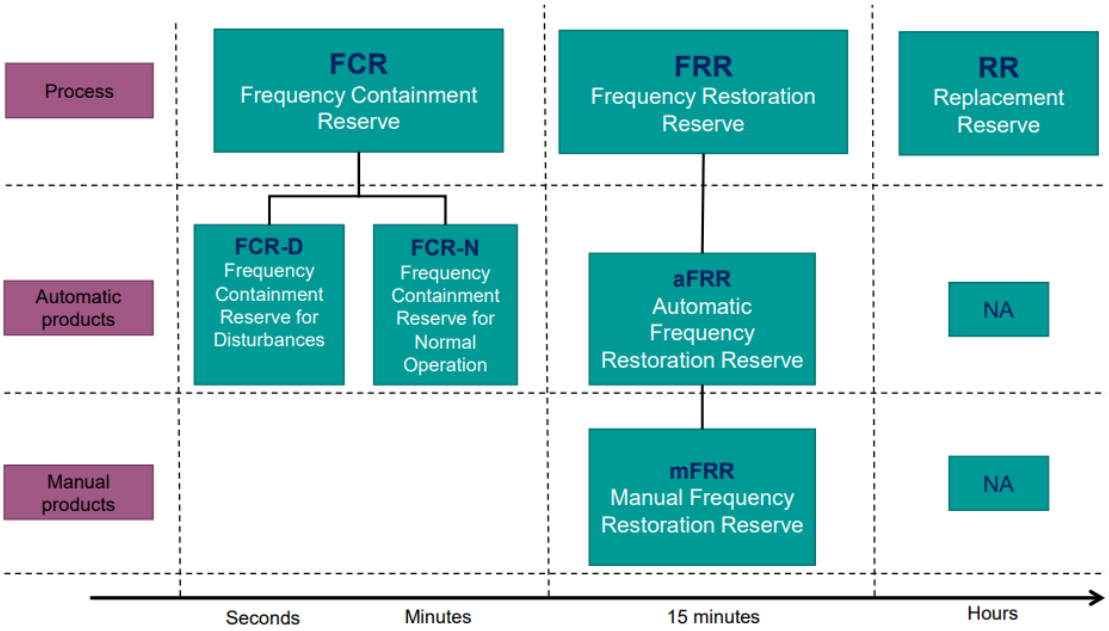

Figure 6. *Frequency control process used in Finland. The frequency control process is divided into three categories. (Fingrid, 2018)*

Frequency Containment Reserves (FCR) are used to control the frequency constantly. Frequency Restoration Reserves (FRR) are used to restore the frequency back to the acceptable limits and to release FCR back to use. Replacement Reserves (RR) aims at restoring activated FRR back to the state of readiness in case of reoccurring disturbance. At the moment RR is not used in the Nordics. (Fingrid, 2019c)

Figure 7 below presents an example of the frequency restoration process.

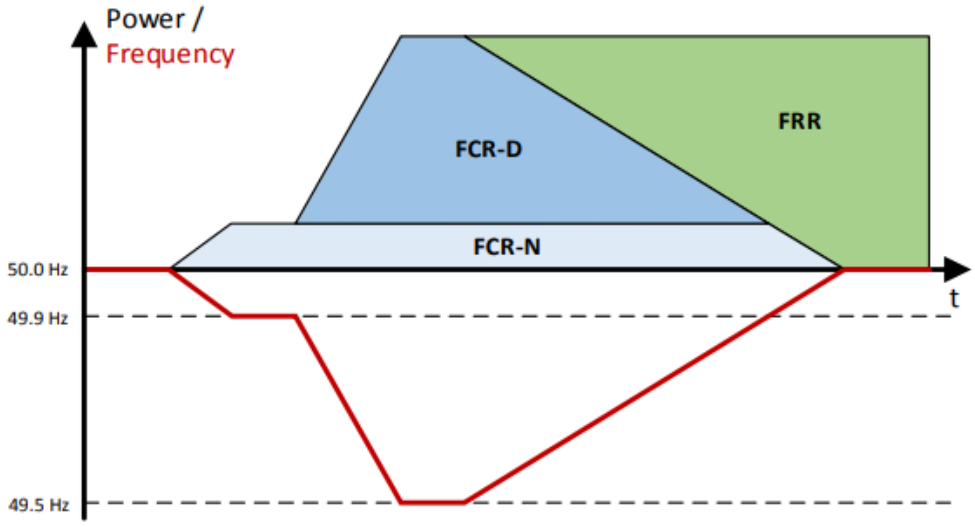

Figure 7. *Frequency restoration process. First reserve to activate when the frequency decreases is FCR-N and the second is FCR-D. (Entsoe, 2017)*

In situation, where frequency remains stable at 50 Hz, the reserves remain inactivated. As frequency begins to decrease, Frequency Containment Reserve for Normal operation (FCR-N) activates. If frequency reaches 49,9 Hz, all the procured volume of FCR-N is activated. In case frequency decreases beyond 49,9 Hz, Frequency Containment Reserve for Disturbances (FCR-D) begins to activate. The full capacity of acquired FCR-D is activated when the frequency reaches 49,5 Hz. Automatic or Manual Frequency Restoration Reserves (aFRR or mFRR) are used to restore FCR-D back to the state of readiness within 15 minutes. (Entsoe, 2017)

Operation of FCR-N and FCR-D is linked to the frequency of the grid and switched on automatically. Full activation time of these reserves can vary from fractions of seconds to minute depending on the product. The duration depends on the frequency of the grid and can be from seconds to hours. mFRR and aFRR are ordered manually by the TSO. Full activation time for these products varies from minutes up to 15 minutes. The duration of the manually ordered reserves can vary between 15 minutes to hours depending on the length of the disturbance. (Fingrid, 2019a)

3. HYDROPOWER

Hydropower is an emission-free and renewable source of energy. Hydropower is described as the most mature, reliable and cost-effective renewable power generation technology available (IRENA, 2012). Hydropower production is based on the hydrologic cycle thus the amount of hydropower generation available is related to the existing hydrological situation.

This chapter focuses on the basics of hydropower and the analysis of Run-of-River hydropower characteristics. Section 3.1 covers the basics of hydropower including presentation of the hydrologic cycle, description of a hydropower unit and electricity generation. Following section 3.2 focuses on hydropower production planning and its characteristics.

3.1 Basics of Hydropower

Hydropower is the largest source of renewable energy in the world (IEA, 2018). Figure 8 below presents the source shares of electricity generation.

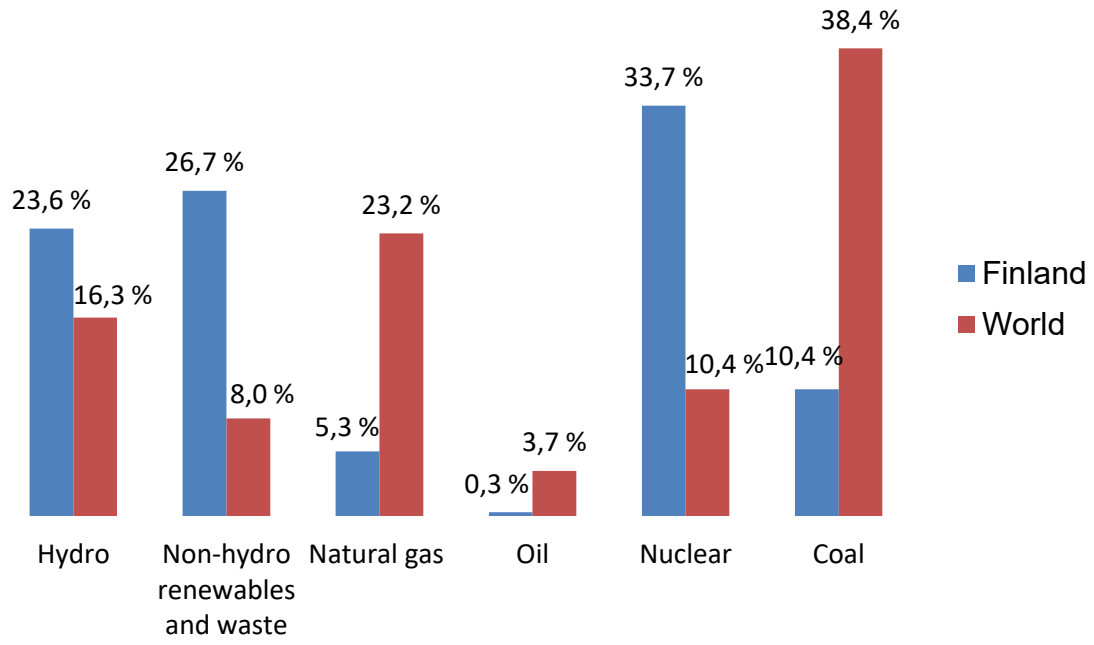

Figure 8. *Source shares of electricity generation in 2016. Red column presents the world's shares (IEA, 2018) and the blue column presents Finland's shares (Energiateollisuus, 2017). The share of hydropower is nearly half of the renewable energy production in the world. In Finland hydropower covers 16.3 % of the total production and 67 % of the renewable production.*

Hydropower produces a low-cost renewable electricity and provides significant flexibility for the grid. The spinning hydropower turbine can be ramped up or down rapidly to provide additional generation or voltage regulation. These are used to ensure that the electricity grid operates within its quality limits (IRENA, 2018). Hydropower also has a considerable role in preventing floods and limiting the descend of the water level in dry periods (IRENA, 2018). Building hydropower has an effect on the river system. The main influence is caused by the construction of water reservoirs and dams. The dams block the natural movement of fishes which can effect on the fish stocks. The impacts are reduced by fish planting and building fish passes. Production of hydropower has effects on the river system caused by the variation in water levels and the changes in discharges. Environmental permits specifies the accepted minimum and maximum water levels and typically the minimum discharge. The regulation limits vary based on the calendar dates or discharge of the water system. The regulation of water limits aims at improving recreational use and preventing floods. (Lummikko, 2017; Energiateollisuus, 2019b)

3.1.1 Hydrologic Cycle

The hydrologic cycle is a continuous water cycle on the earth in every state of matter. The water cycle or hydrologic cycle is a process where the water continuously moves between the surface of the earth and the atmosphere. The process is powered by the solar energy and the gravitation. Figure 9 below presents the water cycle more closely in a fictional catchment area.

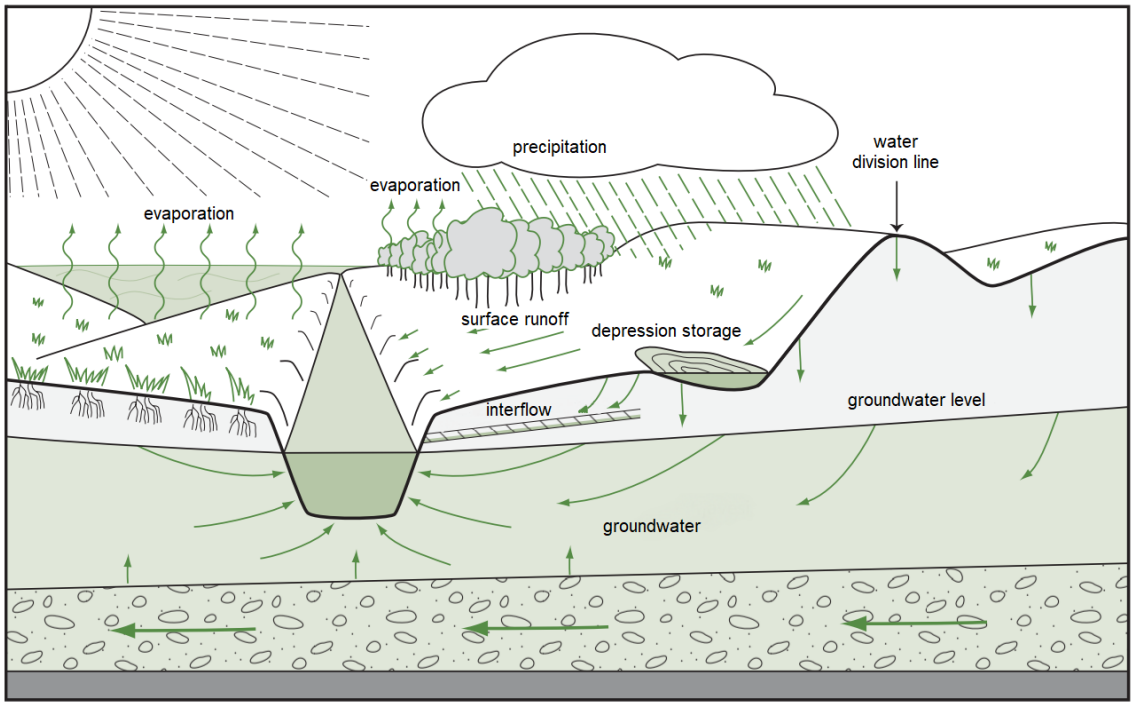

Figure 9. *The water cycle in a fictional catchment area. Adapted from Paasonen-Kivekäs et. al. (2016)*

The water cycle begins from the evaporation of water caused by the solar energy. Evaporation is a process where the liquid water in oceans, lakes, rivers, etc. changes into water vapor. The vaporized water cools as it rises and enters the atmosphere. The condensed water vapor forms clouds as the vapor turns into a small liquid drops. The small droplets of water move around and hit one another forming larger drops. These larger drops become too heavy to be held up and they fall back into the ground as precipitation. The temperature determines the form of the precipitation, it can fall as drizzle, rain, snow and many other forms. (Ghosh and Desai, 2006)

Runoff is the water movement from ground areas to the river and lake systems. The total runoff consists of three types of forms. The surface runoff is the precipitation or snowmelt, that moves as surface water to the lake and river systems. The interflow is the portion of runoff which is absorbed into the surface layer of the ground and migrates to water channels. The last form of runoff is the subsurface drainage. (Paasonen-Kivekäs *et al.*, 2016)

3.1.2 Electricity Generation

The electricity generation of hydropower is based on the potential energy caused by the height difference between the upper and lower water level. The stored water from the upper reservoir is released through the penstock. The water flow rotates the turbine, which is connected to a generator using a shaft. The generated electricity is transmitted to the customers using high voltage power lines (Mäkiharju, 2012). Figure 10 below illustrates this process.

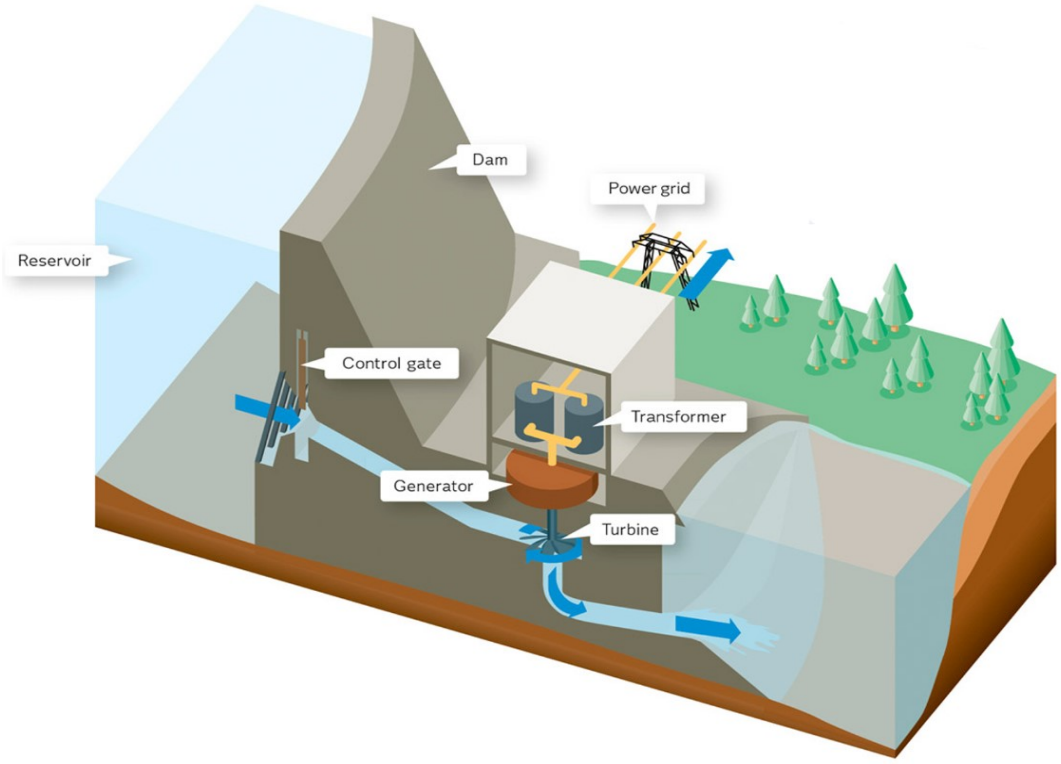

Figure 10. *A general hydropower plant scheme (Vattenfall, 2019). A fundamental part of the hydropower plant, the spillway, is not shown in the figure.*

Spillways are used to bypass the dam in a situation, where the inflow is greater than the maximum discharge capacity of the turbine(s). In the Nordics, spillage is needed typically during the spring floods. The spilling the water wastes energy thus hydropower producers aim at avoiding or minimizing spillage. In practice, spilling is done only in order to control the upper reservoir water level. (Crona, 2012)

The amount of electricity generated depends on the used potential energy of water and the height difference between the upper and lower water reservoir. This height difference is known as the head of the hydropower plant (IRENA, 2018). The potential energy of the water is a function of discharge and head of the hydropower plant. The water stored in the upper reservoir has potential energy *U* [*J*] and can be present with function:

$$U = mgh, \tag{1}$$

where *m* is the mass of water [*kg*], *g* is the gravity acceleration constant [9.81 $^{m}/_{s^2}$] and *h* [m] is the head of a plant. The mass is a product of the density and volume of water ρ [1000 $^{kg}/_{m^3}$] and the volume *V* [m^3]:

$$m = \rho V \tag{2}$$

The theoretical power P_{th} [$^{J}/_{s}$] is division between the energy and time [*s*]:

$$P_{theoretical} = {}^{U}/_{t} \tag{3}$$

With the equations (1) and (2) the theoretical power equation (3) can be presented as follows:

$$P_{theoretical} = {}^{\rho V g h}/_{t}. \tag{4}$$

The volume of the water through a hydropower plant during a certain time can be written as the discharge *Q* [$^{m^3}/_{s}$]. The head of the plant can be expressed as the separation between the heights of the intake water and the tail water. With these modifications, equation (4) is simplified to a form:

$$P_{theoretical} = \rho g Q (h_{intake\ water} - h_{tail\ water}) \tag{5}$$

Hydropower, like any other energy production method, has losses. The losses in hydropower are caused when the water flows through waterways and past the turbine to the lower water reservoir. Most of the losses (11-12 %) are caused by the turbine losses depending on the turbine type and when the water encounters friction in the penstock. The losses are increased by the tail water: how the water moves away from the turbine allowing new water to enter the lower reservoir. Finally, a minor part of the losses (2 %) is caused by the electricity transmission and generation. The total losses of a hydropower plant are 12-14 %. (Førsund, 2007)

Therefore, the actual power P must be scaled with an efficiency factor η which takes the losses into account during the energy conversation:

$$P = \eta \rho g Q (h_{intake\ water} - h_{tail\ water}) \tag{6}$$

In conclusion, the amount of produced electricity depends on the discharge through the turbine, the head of the plant and the efficiency of the energy conversation. Changing the amount of electricity produced is done by altering the discharge of water through the turbine. Water discharging through the dam will have the effect that the head of the plant decreases by lowering the upper reservoir water level and increasing the tail water level. The decrease in the upper reservoir level is an outcome when the discharge of the plant is greater than the inflow. Considerable discharge or spillage causes effect where river resists the flow of the water with the consequence that tail water raises. (Vilkko, 1999; Førsund, 2007)

3.1.3 Hydropower Plant and Turbine Types

Hydropower plants are typically classified on the grounds of the upper reservoir volume and electricity production capacity. These three types are run-of-river hydropower, reservoir hydropower and pumped storage hydropower. All types of hydropower plants can have a broad spectrum of size and capacity. The production capacity can vary from the pico scale (the maximum of 5 kW) to the large scale (greater than 10 MW). (IRENA, 2012; IEA-ETSAP, 2015)

Run-of-river (RoR) hydropower has little or no water storage capability, which means that production is based on the timing and the river flow since nearly all the arriving water must pass through the plant constantly. RoR plants with the capability to store some water are said to have pondage. This pondage allows a short-term (hourly or daily) optimization of the production when it is needed the most. A plant without pondage can schedule production in cases where there is possible to time the incoming water flows from the upper hydropower plant or reservoir. Run-of-river hydropower plants are typically found downstream of a reservoir hydropower plants as one reservoir can schedule the production of multiple downstream ROR plants. Thus, the main starting value for production planning is the inflow rather than the forecasted electricity price. Some river systems have relatively steady inflow while others will experience significant variations in the inflows. (Eurelectric, 2011; IRENA, 2012)

Hydropower plants with a large reservoir behind dams are called conventional hydropower. The reservoirs can effectively store water and act as an energy storage system. The stored water is used when the electricity price is high and stored in times with low demand of the electricity. Large reservoirs enable coupling the electricity generation with times of rainfall or the melting of ice and snow. Typically, the reservoirs are emptied during winter to prepare for the inflows caused by the melting of snow. This inflow is stored to meet the higher electricity demand in the winter. Conventional hydropower is also able to respond nearly instantly to changes in the balance of production and consumption in the electricity grid. This facilitates the low-cost integration of variable renewables into the grid. (Eurelectric, 2011; IRENA, 2012)

The third type is the pumped storage hydropower. Pumped storage hydropower operates with the lower and the upper reservoir. The working principle of pumped storage hydropower is presented below in Figure 11.

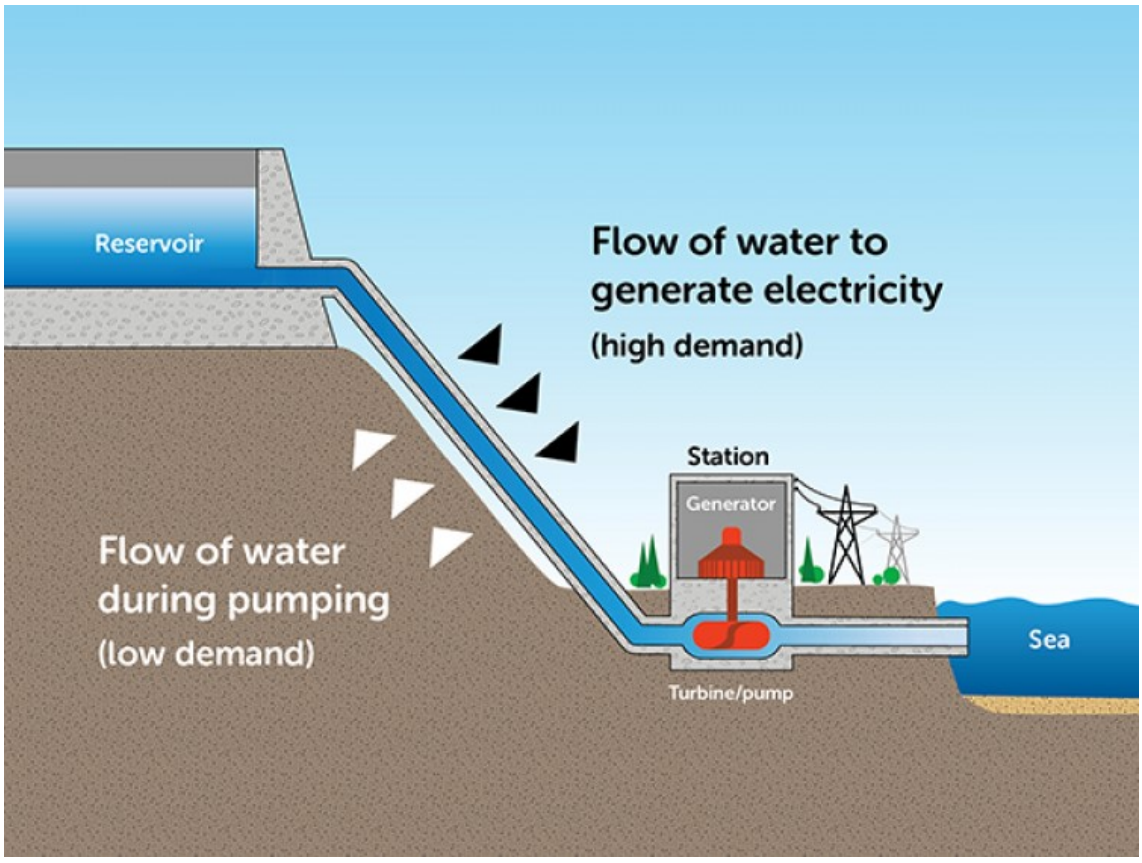

Figure 11. *The principle of a pumped storage hydropower plant (Energy Storage News, 2017). The times of lower demand for electricity are used to pump the water from the river or lower reservoir back to the upper reservoir. This stored water is used to generate electricity in the hours of high demand for electricity. Pure pump storage hydropower has no natural inflow and has human-made upper and lower reservoirs. (Eurelectric, 2011)*

The main benefit of the pumped storage hydropower is its ability to store energy on a large scale thus providing valuable grid stability services. Pumped storage hydropower is much less expensive than Li-ion and lead-acid batteries. The overall efficiency of a pure pump storage hydropower plant is in the range of 70-75 %. Relatively low efficiency is compensated by the flexibility these plants can provide. (Eurelectric, 2011; IRENA, 2012)

The three main turbine types typically used in hydropower plants are Kaplan, Pelton and Francis. Kaplan turbines are typically used in Run-of-River hydropower because of its large flow-rate and small head characteristics. Kaplan turbine rotors are the only type of turbines with the ability to set the stagger angle. The typical maximum efficiency of a Kaplan turbine is approximately 94 %. Pelton suits well in applications where the head of the plant is high and discharges are low. It is the only impulse type hydraulic turbines in common use on the present day. The maximum efficiency of a Pelton turbine is 90 %. Last turbine type is Francis. It has wide operation range thus it suits well in applications with either high or low head of the plant. Francis turbine has the highest efficiency, around 95 %. (Dixon and Hall, 2013; IEA-ETSAP, 2015) Figure 12 presents the three turbine's load-efficiency-curves.

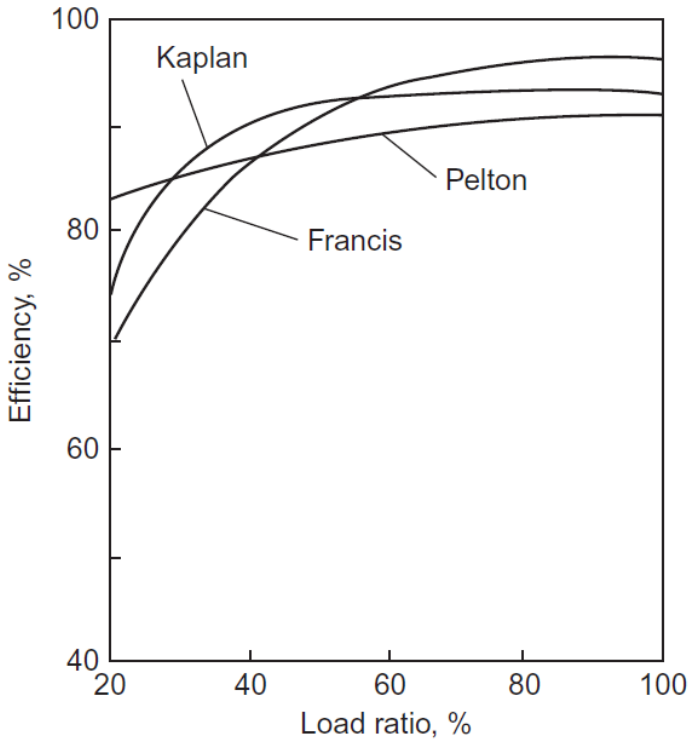

Figure 12. *Efficiency curves of Kaplan, Francis and Pelton turbines (Dixon and Hall, 2013).*

The terrain in Finland is relatively flat. Thus, the head of hydropower plants is typically low. The main turbines used in Finland are Francis and Kaplan. Especially Kaplan is commonly used in Finland because of its flat and high-efficiency curve. Kaplan is suitable for deviating the discharge without markable changes in the efficiency factor. This allows the peaking and cycling production. (Antila, 1997)

3.2 Hydropower Production Planning

Hydropower production planning requires accurate forecasts of the inflow in addition to the electricity price forecast (Bai *et al.*, 2016). The water levels in reservoirs and the future inflows have a fundamental role in the optimization of hydropower (Mäkiharju, 2012). This section focuses on the key components of the planning and operation of a river system.

3.2.1 Reservoir and Inflow

Over 300 lakes or reservoirs are regulated in Finland. These lakes and reservoirs are connected to river systems with hydropower plants or dams with the ability to regulate the discharge. Regulation of watercourses is a term for altering the discharge through the water structures in order to meet the predetermined targets for the water resource management. The most common target for the regulation is to enable production of hydropower, while the most important target is the

flood control. The other targets are advancing log floating or water traffic, water supply, recreational use, fish breeding, soil reclamation and water conservation. (Finnish Environment Institute, 2019b)

The basis for the regulation of a lake, reservoir or river system is the permits subject to the Water Act. These permits define the limits of the water level and discharge. These limits must be taken into account in the planning and operation of the river system. (Finnish Environment Institute, 2019b) The water levels and discharge limits are typically determined based on calendar dates. One typical characteristic is a mandatory water level draw-down before flooding in the spring. This draw-down is preparation for the increasing inflows during snow melting. The draw-down is calendar based and it is done typically during late winter or early spring. This might not be suitable in the future because snow melting decreases and flooding occurs earlier during the winter. (Veijalainen *et al.*, 2010)

Preparation for flooding is illustrated in Figure 13 below.

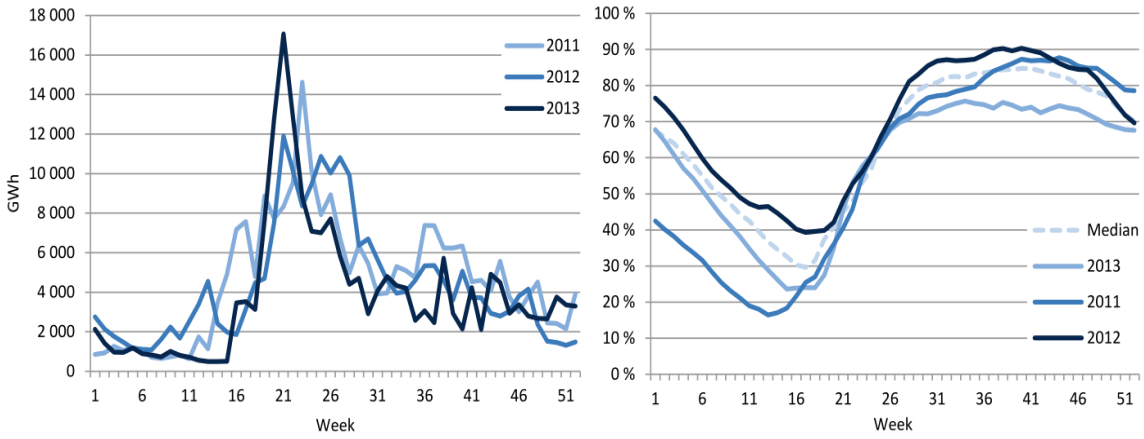

Figure 13. *Effective inflow to the reservoirs is presented on the left-hand side. On the right is the capacity of the reservoirs in the Nordics. Lowering the reservoir levels are seen starting on the first week of each year. The lowest point of water reservoirs is reached typically during April and May. Peaking in inflows caused by snow melting is seen usually later from April till early June. Heavy inflows fill the reservoirs to full capacity of 90 %. (Nordic Energy Regulators, 2014)*

The inflow is based on the hydrological cycle described earlier in Section 3.1.1. The inflow into the reservoir consists of precipitation and runoff. Evaporation and accumulation reduce the amount of inflow water. (Paasonen-Kivekäs *et al.*, 2016) Finnish Environmental Institute forecasts and monitors inflows in Finland. The system is based on hydrological watershed models. The system simulates the hydrological cycle using meteorological and hydrological data. As a result, forecasts are created for 500 water levels and discharge observation points that cover 86 % of the area of Finland. (Vehviläinen and Huttunen, 2001; Finnish Environment Institute, 2019c)

Climate change causes shift in the inflows. In the winter period from December to February, inflows are expected to increase 34-165 % in the years 2040-2069. Large percentual changes are

explained by typically low inflow during winter thus even moderate increase becomes more obvious. The inflow during spring is expected to decrease in the south, west and central Finland because snow cover is thinner, and inflows caused by snow melting are smaller. Snow is expected to melt entirely during spring causing inflows to increase by 6-19 % in northern Finland. This causes inflows to decrease during summer by 13-31 % in norther Finland. Earlier springs in the south cause drought in the soil leading to a decrease of the inflows by 16-25 % in the summer. (Veijalainen, Jakkila and Nurmi, 2012)

Managing the reservoirs requires estimating of the inflow. This is emphasized when relatively small reservoirs are managed. Reservoirs are divided into two categories depending on their volume. A seasonal reservoir is a large reservoir which is filled once or twice a year during the spring flood. A plant reservoir is considerably smaller than the seasonal reservoir. (Vilkko, 1999)

Hydropower producers monitor their reservoir levels constantly. Monitoring is crucial in order to obey boundaries given by the permit and to maximize the head of the plant. Real-time monitoring of water levels and outflow enables accurate estimation of the inflow if reservoir total volume is known. A reservoir with smaller storage capacity reacts to changes in the inflow or outflow more rapidly than a larger reservoir. The change rate of the reservoir level depends also on the current reservoir level. Reservoir level and volume are not linearly dependent. This effect is demonstrated in Figure 14.

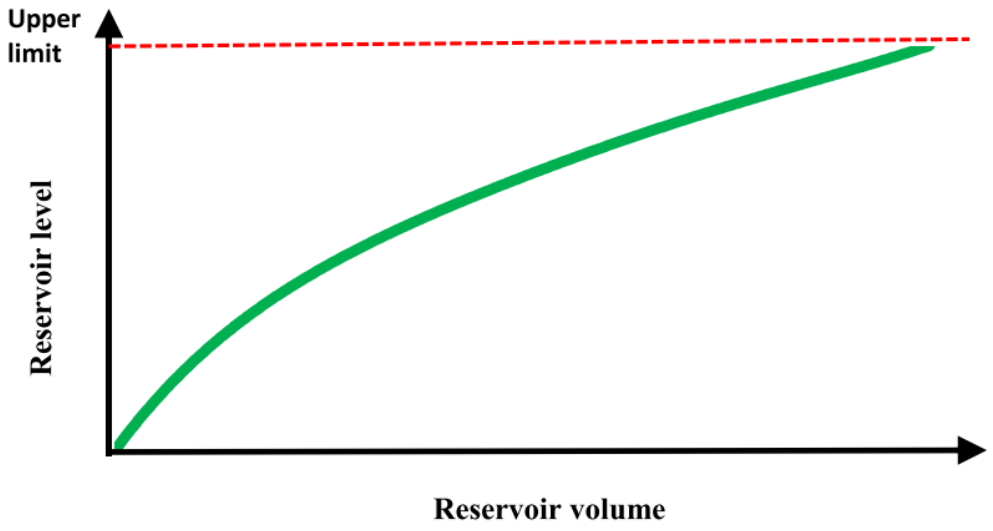

Figure 14. *Example of a hydropower plant's reservoir volume in relation to the reservoir level. The filling and emptying speed of the reservoir depends on the reservoir level. In this example, the filling speed is greater when the reservoir is nearly empty. (Tuovinen, 2019)*

A precise understanding of the reservoir's volume and the outflow from the reservoir makes possible to calculate the exact inflow into the reservoir. This is useful in estimating inflows in reservoirs that have large natural inflows. (Tuovinen, 2019)

The volume of the reservoir can be determined with for example by using hydrographical measurements or statistical data. The hydrographical measurements are done with depth-sounders to determine the shapes of the reservoir beds. With the knowledge of the reservoir beds, the total volume of the reservoir can be calculated (Furnans and Austin, 2007). The volume of the reservoir can be estimated also by calculating the water level change and the difference between inflow and outflow. The water balance equation is as follows:

$$x_t = x_{t-1} - Q_t + q_{upstream} + w_t, \tag{7}$$

where x_t is the current reservoir content, x_{t-1} is the reservoir content in the previous time step, $q_{upstream}$ combined with w_t is the inflow to the reservoir and Q_t is the outflow from the reservoir (Souza, 2012).

3.2.2 Head Effect and Tail Water

The production of the hydropower plant is not linearly dependent on the discharge through the turbine(s). The production of the electrical power increases until it reaches its peak. After the peak, the production may even start to reduce due to the decrease of the plant's head. The main reason for the decrease is that the tail water typically rises during high discharges. Figure 15 is presented the change of water energy content as a function of discharge through a turbine.

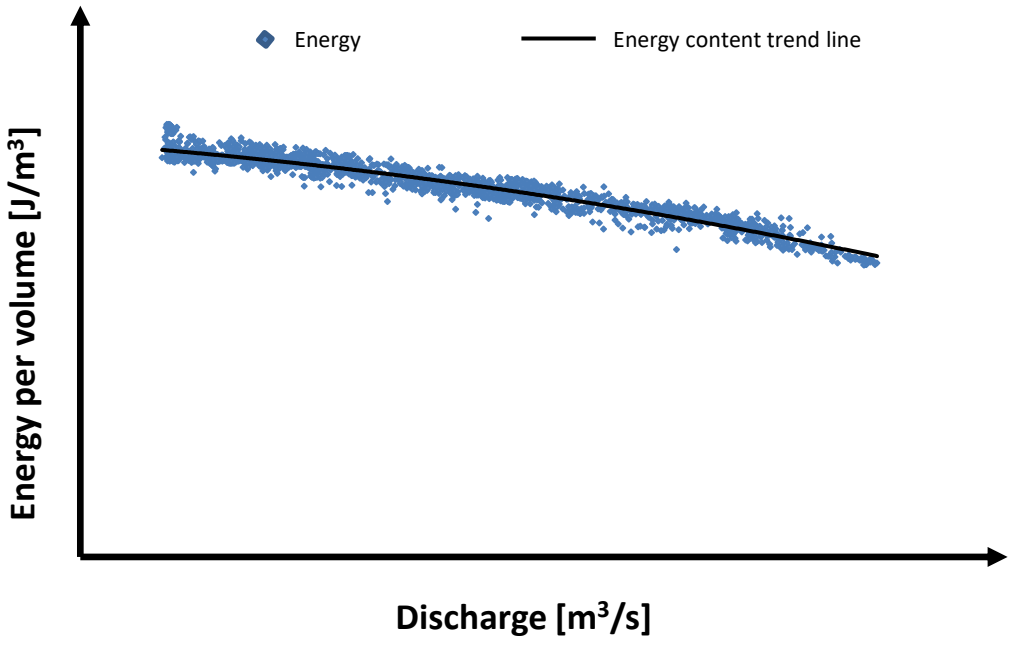

Figure 15. *The change of water energy content as a function of discharge through turbine according to statistical data of an example hydropower plant. The decrease in the energy per volume is caused by the decreased head of the plant.*

The turbine efficiency factor diminishes as well during high discharges. The combined efficiency factor can be increased by starting another turbine so high discharge is divided more effective between turbines. Low discharges are optimally operated wit only one turbine. Figure 16 below demonstrates the efficiency curves of the three turbine hydropower station. Generation output starts to decrease as the water level lowers locally near the turbine intake. Starting up another turbine avoids the decrease in the production efficiency. Therefore, it recommended to use the turbines in the optimal production zone and start up a turbine at the intersection point of two efficiency curves. (Vilkko, 1999)

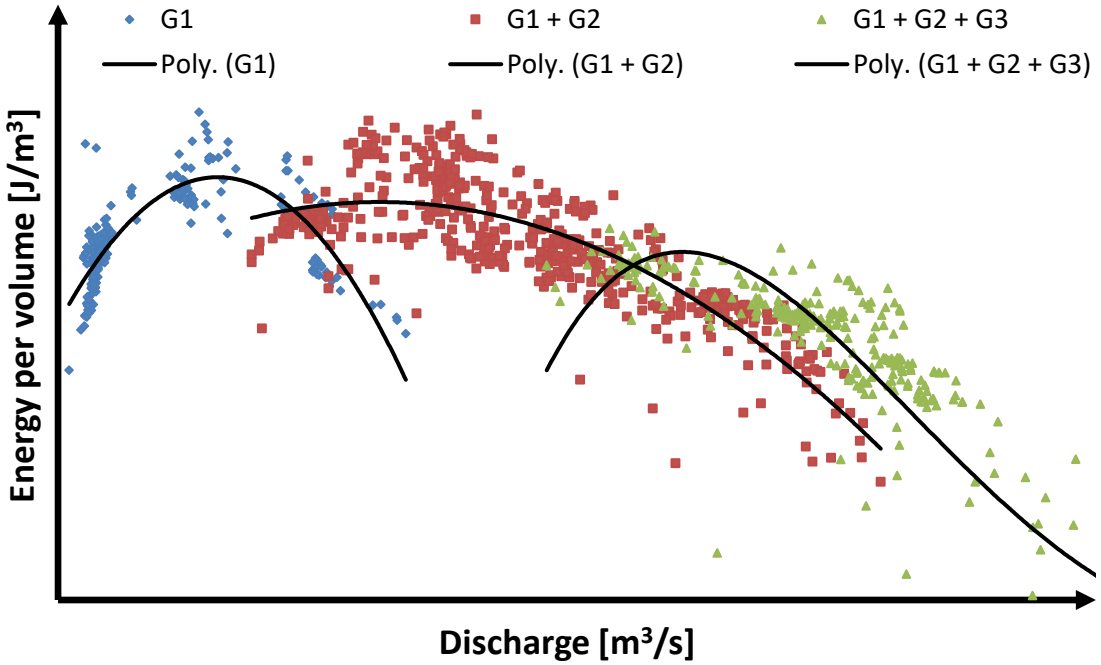

Figure 16. *The efficiency curve of the combined three generators as a function of discharge according to statistical data. Three turbines combination has lower energy per volume than achieved with one turbine. This is caused by the decrease in the head of the plant during high discharges of the plant.*

The water level below a hydropower plant is called tail water. The river tends to resist high discharges caused by the spillage or substantial production of electricity. This causes the tail water to rise. The efficiency of the hydropower plant decreases because higher tail water lowers the head of the plant. (Vilkko, 1999)

The behavior of the tail water can be modeled by linearizing the tail water as a function of the total discharge through the turbines and spillways of the plant. Figure 17 below demonstrates a linearization model of a hydropower plant's wail water level.

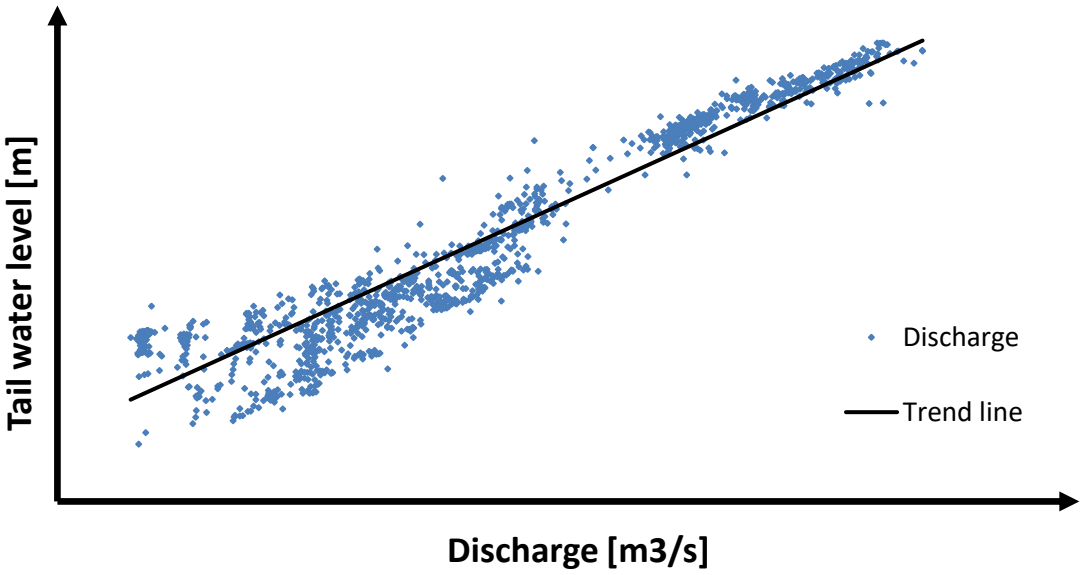

Figure 17. *Linearization of a hydropower plant tail water according to statistical data. The figure illustrates the rise of the tail water during high discharges.*

3.2.3 Water availability

As mentioned before, RoR hydropower stations located in the same riverbed are hydraulically coupled. Thus, the water released from the upper reservoir forms most of the inflow to the latter reservoir. The time delay from the upper station to the lower station must be known in order to be able to make realizable production plants and to keep the lower station water levels within acceptable limits. This time delay between stations depends on the distance between stations. More closely the challenge is to model how a certain wave caused by an increase or decrease of discharge travels along the riverbed. (Vilkko, 1999)

The most commonly used way to model delay between hydropower stations is to consider a constant delay. The mathematical presentation of water balance for hydropower plant i can be presented as follows:

$$V_i^t + (Q_i^t + S_i^t) - \sum_{j \in M_i} \left(Q_j^{t-\tau_{ij}} + S_j^{t-\tau_{ij}} \right) = V_i^{t-1} + I_i^t \quad (8)$$

, where

V_i^t is the reservoir of hydropower plant i at the end of time step t

Q_i^t is the turbine discharge of hydropower plant i at time step t

S_i^t is the spillage of hydropower plant i at time step t

M_i is the set of hydropower plants immediately upstream of hydropower plant i

τ_{ij} is the water delay between upstream hydropower plant j and downstream plant i

I_i^t is the natural inflow to hydropower unit i at time step t. (Souza, 2012)

In reality, cascaded river systems water released from the upper reservoir may split into several parts, which may arrive at the latter hydropower plant in different time steps (Souza, 2012). This phenomenon is demonstrated in Figure 18 below. The figure shows that water released from the upper hydropower plant in τ_p arrives at the lower reservoir from time steps $(\tau_p + 1)$ to $(\tau_p + 4)$.

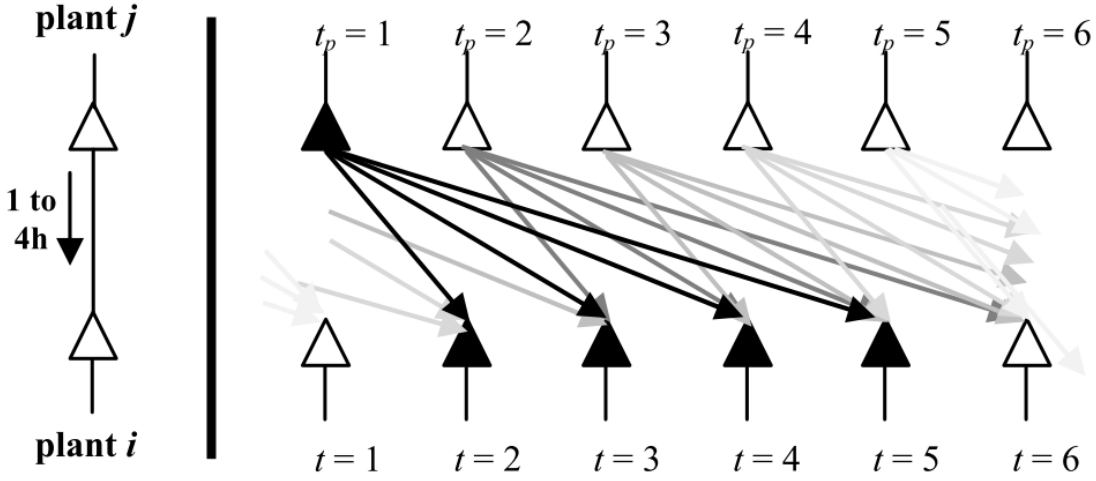

Figure 18. *Streamflow routing effect between two hydropower plants. Arrows represent portions of moving water in the river system. This approach lead to a streamflow routing curve. (Souza, 2012)*

The streamflow routing curve is a factor that gives the cumulative percentages of the water released from the upper hydropower plant at time step t_p that reach the subsequent hydropower station up to each time step $(t = t + k)$ until the whole amount of water released has arrived. The factor κ varies from the first portion of water arriving at the lower plant to the time where cumulative arrived water has reached 100 %. The water balance function with the factor κ can be presented as follows:

$$V_i^t + (Q_i^t + S_i^t) - \sum_{j \in M_i} \sum_{\kappa=0}^{\tau_{ij}^t} \kappa_{ij,k}^t \left(Q_j^{t-\kappa} + S_j^{t-\kappa}\right) = V_i^{t-1} + I_i^t \quad (9)$$

, where the factor $\kappa_{ij,k}^t$ is the portion of water released from the upper hydropower plant (j) at the previous time step $t_p = t - k$ that reach the subsequent hydropower plant (i) at time step t. (Souza, 2012)

3.2.4 Production Scheduling

Hydropower planning horizons are divided into three with respect to the time frame: short-term, medium-term (mid-term) and long-term. The main idea is that plans for longer periods are inputs to the shorter planning. Planning focuses on maximizing the profits on a certain planning horizon

by timing the production when it is the most profitable. Planning uncertainties are caused by inaccurate forecasts of the inflow and market price. (Fosso *et al.*, 1999; Vilkko, 1999)

The long-term planning of hydropower covers the time horizon from one year to decades. The long-term plans facilitate decisions regarding the controllability and availability of hydropower. These decisions include questions about whether investing in an additional hydropower capacity or minimizing the costs of long capacity unavailability caused by maintenance. The electricity price has a strong dependence on the weather conditions. The weather forecasts are reliable for a few days forward but not on a yearly basis. Thus, accurate inflow and electricity price forecasts are not available for long-term planning. The long-term planning of hydropower considers larger phenomenon such as climate change or changes in the power production system caused for instance political decisions. Key outputs from long-term planning of hydropower are support for decision making of hydropower investments and guidelines to manage hydro reservoirs. (Antila, 1997; Fosso *et al.*, 1999; Scharff *et al.*, 2014)

The time horizon of one week to 18 months is called mid-term or medium-term planning. Mid-term plans are typically made in the weekly resolution providing an endpoint for reservoir level planning required in short-term planning. Mid-term planning inputs are current the reservoir level and the forecasted inflow and the electricity price. The uncertainty of the forecasts increases when the forecasting horizon is greater. This means that the uncertainty of the mid-term planning also increases when using longer planning horizon. Available energy is calculated from the start and end points of reservoir level. Available energy is then allocated to the time period so that the target set at the end level of the reservoir is reached. (Fosso *et al.*, 1999; Scharff *et al.*, 2014)

Short-term plans are made with hourly resolution from the following day to two weeks ahead. The objective for planning is to maximize the profits by allocating the available production to the most profitable hours. Short-term models take into account a complex model of the cascaded river system. Each plant and river system have different properties and constraints that affect the planning of the production. (Wangensteen, 2006) It is possible to make short-term forecasts with sufficient accuracy for inflow and the electricity price. The forecasted values are treated as the right ones during planning. The planning is carried out again when forecasts change noticeably. (Antila, 1997) Mid-term plans set the boundary conditions for short-term planning. In practice, mid-term sets the targets for reservoir levels which are met with short-term planning. Boundaries set by mid-term plans should not decrease the flexibility of managing possible changes in the inflow. (Fosso *et al.*, 1999)

3.2.5 Decision Making Process

The operational decision-making process of a Nordic hydropower producer is presented below in Figure 19.

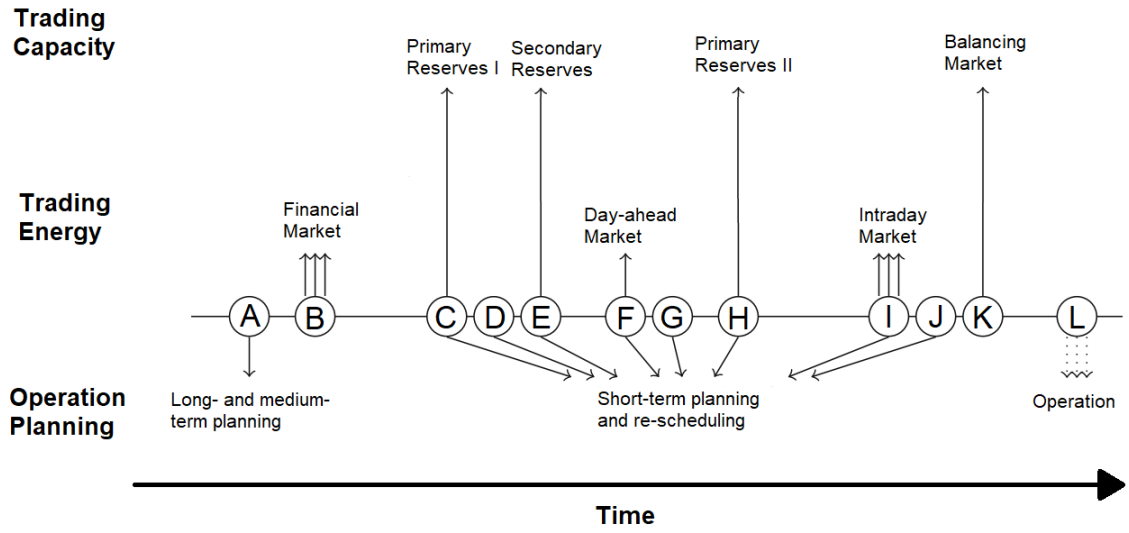

Figure 19. *Decision points of a Nordic hydropower producing company. Adapted with modifications from Scharff et. al. (2014). A single arrow marks a discrete decision and multiple arrows present a sequence of decisions within a time interval. An example of a sequence of decisions is trading on a continuous trading platform such as Elbas.*

A. Long-term and mid-term planning of production, *from year to decades ahead*
B. Trading on the financial markets, *years ahead*
C. The bidding process for the yearly market of frequency containment reserves, *once a year in the fall for next year period*
D. Short-term planning of production, *weeks ahead with hourly resolution*
E. The bidding process for Fingrid's balancing capacity market, bidding once a week for the period of the following week (only if Fingrid decides so)
F. Bidding on the Day-ahead market, once a day for the following day
G. Short-term production planning, *a day ahead*
H. The bidding process for hourly frequency containment reserves, *a day ahead*
I. Intraday market, *hours ahead*
J. Self-balancing, *hours ahead*
K. Bidding for the balancing market, *hours ahead*
L. The real-time operation, *the hour of delivery*

Figure 19 illustrates that hydropower production planning is a continuous process. The planning begins from the long-term plans and ends with the real-time operation of the units. Decision steps listed above are valid in all hydropower generating companies in the Nordics. The company's size

and long-term supply contracts define the boundary conditions of the company's individual decision-making process.

The focus of this thesis is on the intraday operation and planning of hydropower after the Day-ahead market results are published. Therefore, the decision points from G to L are analyzed more carefully. The actions taken in earlier points might constrain allowed actions in the intraday operation and planning. Thus, earlier stages of the planning must be taken into account. Bidding in the annual market of frequency containment reserves is an example of a constraint that affects the intraday operation. Capacity sold to the annual frequency containment market is not available in trading in other reserve markets nor balancing power market. This means that revenue lost from one physical market should be less than the revenue gained from another market (Wangensteen, 2006). Coordinated bidding is a term that considers all possibilities in the other markets as well when bidding into one market. If other market places are not considered, the bidding is called sequential bidding (Kongelf and Overrein, 2017).

Decision point G in Figure 19 illustrates the short-term production planning. At this point, the detailed production plans are made based on the realized amount of energy sold to the day-ahead market. The production plans are made for each hydropower plant and production unit. The production plan aims at operating the production unit at the optimal power transfer ratio and to minimize the own generation costs. Some uncertainties concerning decision point G are electricity prices in the intraday market, the balancing power market price and the power plant outages. Decision point H includes the tendering process for the hourly primary reserves. In this point, the producers need to decide the capacity and price for reserves offered to TSOs. The aim is to maximize the expected profits from the reserves. (Scharff *et al.*, 2014)

Whether to buy or to sell energy on the intraday market are continual decisions made in the point I. As stated earlier, hydropower is a flexible form of electricity production thus it is suitable for adjusting commitments sold to the day-ahead market. Adjusting commitments can be done by trading in the intraday market. The intraday market prices can deviate from the day-ahead price when the hour of delivery comes closer. Errors in the forecasts, for example the wind power generation or consumption, increases or decreases the demand for electricity leading to variation between intraday and day-ahead price. The deviations enable opportunities to profit from re-scheduling the production plans of the hydropower station. Adjusting the production plan to match the commitments on the intraday and day-ahead markets are done in the decision point J. (Scharff *et al.*, 2014)

The decisions regarding offers to the balancing market are made in the point K. Offers include the capacity and price for up- and down-regulation of production. The capacity available for regulation can be determined after the final production plan is made based on the decisions made in points from G to J. All bids done to the balancing market have to be linked to a specific group of power plants. (Scharff *et al.*, 2014)

The operative decisions in real-time are made in the point L. The operator follows the final production plan during the delivery hour. The frequency containment reserves are activated automatically but accepted offers to the regulation market need to be activated manually. (Scharff *et al.*, 2014)

The operative decision-making process of a hydropower producer is a complex task. Different trading and scheduling decisions are dependent on each other. This significantly increases the complexity of the decision-making process. (Scharff *et al.*, 2014)

3.2.6 Optimization of Hydropower

Optimization is described as the science of determining the most optimal solution to mathematically specified problems. The aim of the optimization is also defined as choosing the most optimum elements from a certain set of alternatives available. There are three main kinds of optimization suitable for hydropower production planning, linear programming, nonlinear programming and dynamic programming. (Snyman, 2005)

Linear optimization has the capability to efficiently solve large-scale problems and convergence to global optimum (Labadie, 2004). Linear programming is widely used in the hydropower optimization even though power generation function is nonlinear. Most of the cases it is accurate enough to assume a linear or piecewise linear dependency between the power generation and the discharge. The head effect is also often ignored, particularly if the head variations are small compared to the reservoir level (Kervinen, 2010). These simplifications shorten the calculation times and enable the use of simpler software. Linear optimization model can be written:

$$\begin{aligned} &\max_x \; c^T x \\ &\text{s.t. } Ax \leq b \\ &\text{and } x \geq 0, \end{aligned} \tag{10}$$

where x is a vector of variables, c is an objective vector, b is a vector of constants related to the constraints and A is a constraint matrix.

Optimization may need binary variables for representing some nonlinear or nonconvex terms of the model. Optimization using binary variables is called Mixed-Integer-Linear Programming (MILP). For example, discharges below a certain level might not be feasible because the turbine can break because of the cavitation. In these cases, the discharge variable may be either zero or above a certain level. The binary variables increase the solving time of the optimization significantly. (Pelkola, 2018)

Linear programming is a useful mathematical method to solve a multitude of problems. Linear programming's challenge is that the objective function and constraints must be either linear or possible to be modified as linear. Nonlinear programming offers a solution for problems that cannot be transformed into linear. Nonlinear programming can be written as follows:

$$\max_x f(x)$$
$$\text{s.t. } g(x) \leq b \quad (11)$$
$$\textit{and } h(x) = c,$$

where $f(x)$ is an objective function, $g(x)$ is the inequality constraints and $h(x)$ is the equality constraints.

Nonlinear programming is useful in the optimization of hydropower if the turbine head behaves in a nonlinear way. Catalão et. al. (2006) state that it is crucial to include the nonlinear elements of hydropower in the optimization process in order to increase profits on a liberalized electricity market as they create more value compared to the linear optimization (Catalão *et al.*, 2006). Other studies suggest that with nonlinear programming it is possible to reach better results than with linear hydropower programming (Catalão and Mariano, 2007). Solving nonlinear programming requires derivative of matrix. Also, the algorithms will only find the global optimum if certain convex prerequisites are fulfilled. (Labadie, 2004)

Dynamic programming addresses sequential decision problems. It is a potent algorithmic paradigm in which the optimization problem is first divided into smaller sub-problems and then solving them from the smallest to the largest. The main idea behind dynamic programming is that the answer to smaller problems are used to solve the larger ones. The problem of dynamic programming is longer computing times compared with linear or nonlinear programming. (Dasgupta, 2006) This problem is often referred as the curse of dimensionality. In practice, it means that when the dimensionality increases causing the volume of space to grow fast which leads to increased computing times. (Bellman and Dreyfus, 1966) Hence compromises needs to be made regarding the accuracy and resolution when using dynamic programming. (Dasgupta, 2006)

Dynamic programming can be stated as follows:

$$max_{u(t)} G\left(x\left(t_f\right), t_f\right) + \int_{t_0}^{t_f} F(x(t), u(t), t)dt \quad (12)$$

such that

$$\dot{x}(t) = f(x(t), u(t), t)$$
$$g(gx(t), u(t), t) = 0$$
$$h(x(t), u(t), t) \leq 0$$
$$x(0) = x_0$$
$$x_L \leq x(t) \leq x_U$$
$$u_L \leq u(t) \leq u_U$$

where $x(t)$ is a state variable for example energy or water content, $u(t)$ is a control variable, which is in this case the total discharge of the plant including spillage.

4. ANALYSIS OF THE RIVER SYSTEM

The studied river system covers a catchment area of 27 046 km^2. Lakes cover 11 % of the catchment area and the main channel erupts to the sea. This thesis focuses on the operation and planning of the main channel which is understood as the river starting from the last large reservoir and ending to the tail water of last hydropower plant. The main channel consists of four hydropower plants.

Section 4.1 introduces the principle of the Governance rule. Section 4.2 analyses the reservoirs and hydropower units located in the studied river system. The governance rule contains restrictions for the usage of the studied river system. These constraints regarding the daily operation and planning of the river system are presented in section 4.3. Section 4.4 analyses the uncertainties in the planning and operation. The calibration of the hydropower turbines' discharge measurement was conducted by an outside company. The results of the measurements are presented in Section 4.5. Section 4.6 describes the features of the installed water flow meters and Section 4.7 presents the data available for use in this thesis.

4.1 The Governance Rule

The hydropower units in the river system are owned by multiple companies. All the companies have different strategies to plan and operate their hydropower units. Despite this, the hydrologic balance must be maintained within certain limits. A set of rules have been ordained to aid the co-operation of the river system. These guidelines are called the Governance Rule. It gathers the necessary regulations together into a single guideline document for the river system. Each Governance Rule is determined to a specific river system and is not universal.

The Governance Rule assists the parties in co-operation of the hydropower units in the river system. The Governance Rule illustrates the area that consists of the hydropower units, the catchment areas, the reservoirs and inflow streams resulting in a description of the whole river system and its characteristics. The Governance Rule begins with a brief overview of the river system. It continues with a specification of the regulation limits and ends with a specific discharge regulation for some hydropower units in the river system. Rules are obeyed constantly in times of normal operation. Special circumstances such as spring floods, unexpected heavy inflows or extreme droughts are exceptions, that need to be handled case-by-case. Exceptions may affect the regulation limits, for instance, the obligation of minimum discharge can be lowered or temporarily removed in cases of serious droughts. The constraint regarding the planning and operation of the river system is presented in Section 4.3.

4.2 Reservoirs and Hydropower Units in the River System

The river system studied in this thesis consists of eight hydropower units and five large reservoirs. An illustration of the studied river system is presented in Figure 20 below.

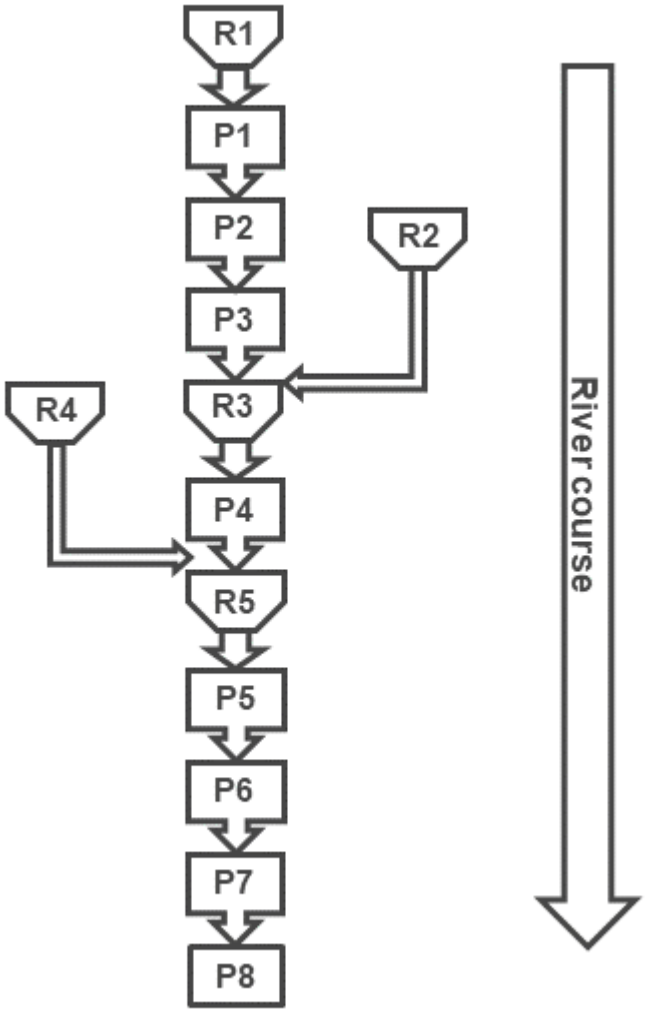

Figure 20. *Illustration of the studied river system. The hydropower plants are marked with letter P and the large reservoirs with letter R. Hydropower stations* P1-P3 *are operated by actor* A*. The rest of the units are operated by actor* B*.*

Reservoir *R1* is regulated by actor *A* since they operate the units below the reservoir. Actor *B* regulates the reservoirs *R3* and *R5*. Operation of the upper hydropower unit has a significant effect on the operation of the lower unit. Thus, the operator of plats *P1 – P3* sends their average planned discharges to the operator of the lower plants. In practice, the operator of *R1, R2* and *R4* inform daily their average discharges to the regulator of reservoirs *R3* and *R5*. Finnish Environmental Institute forecasts inflows to reservoirs and portions of the river between hydropower units.

Hydropower units *P2* and *P3* are typical RoR units, which follow the discharge of *P1*. Unit *P4* is a conventional hydropower plant located between two large reservoirs. Unit *P5* is used for regulation of reservoir *R5*. Unit *P6* is a pure RoR plant without a reservoir. Units *P7* and *P8* are RoR plants with small capability to store water due to a minor reservoir, allowing short-term regulation.

This thesis focuses mainly on analyzing the river section between plants *P6* and *P7* because it is the most challenging to model and operate. It is challenging because of the long distance and noteworthy run-offs between these units. This section of the river is presented in Figure 21 below.

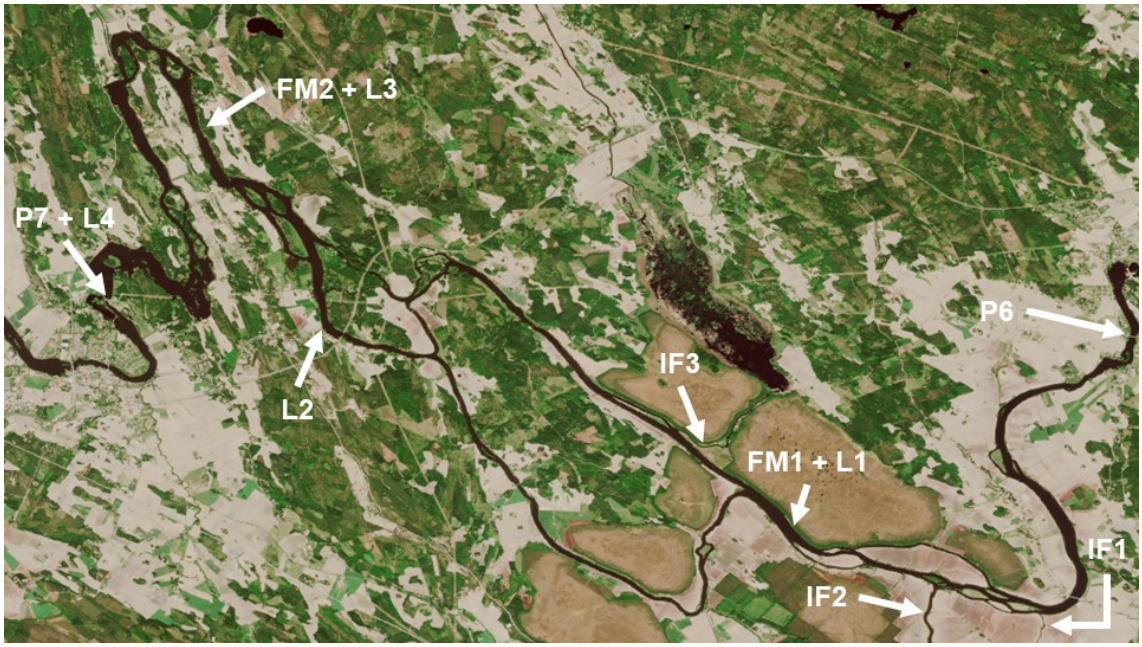

Figure 21. *The river section between hydropower units P6 and P7. The locations of the water level measurements are marked in the figure with L1- L3. The two water flow meters are marked with FM1 and FM2. The three side streams are marked in the figure as IF1-IF3. Image adapted from Finnish Environment Institute, (2019a). Original satellite image from USGS/NASA Landsat Program*

Inflow between units *P6* and *P7* consists of three side streams *IF1, IF2* and *IF3* marked in Figure 21 and run-offs. *IF2* forms roughly half of the inflow. The discharge of *IF2* is estimated with a water level-to-discharge curve by the Finnish Environmental Institute. This estimation is not very accurate in practice, especially in times when the river system has ice cover. *FM1* and *FM2* are used to mark the locations of the water flow measurements. The locations of the water level measurements are marked in the figure with *L1*, *L2* and *L3*.

4.3 Constraints

All the large reservoirs in the studied river system have regulation limits for the highest and lowest water level which vary according to the season of the year. Daily operation and planning must comply with these regulation limits. The river system between units *P5* and *P8* has also regulation

limits that affect the operation and planning. The daily average discharge of unit *P5* must not be less than 30 m^3/s. Reservoir *R5* has regulation limits for the highest and lowest water level. Unit *P6* is a RoR type of hydropower plant. It has the same discharge as unit *P5* with approximately an hour delay. Unit *P7* regulation limits are linked to two water level measurements. The small upper reservoir is measured with *L4* which is in the intake of the unit *P7*. The second measurement *L3* is located 11 kilometers upstream from the unit. The both water level measurements have upper limits stated in the Governance Rule. The intake reservoir has a technical lower limit due to the physical constraints of the plant. Unit *P7* does not have constraints for discharge. The daily average minimum discharge is set in The Governance rule for unit *P8.* Also, the upper reservoir has limits for the highest and lowest water levels. (UPM Energy Oy, 2019)

The units in the river system have two different operating principles. Units can be operated by planned energy or planned discharge. The operation of a hydropower unit with planned discharge may cause energy balance error, which leads to balance costs. In the other hand, units operated by planned energy may cause deviations between planned and realized discharge. If the modeling of unit's intake water level, tail water level and efficiency curve are flawless, there should not be a difference between the planned and realized production of energy or discharge. In practice this is impossible. When plant behaves differently from what is planned, effects can be seen with equation (6). If the head of the plant is less than planned, the same amount of produced energy requires greater discharge. This effect cumulates in the long run, unless the production plan is changed. Energy content per volume is the key factor when choosing the operating principles. If the energy content is low, the error between modeled and realized production energy will not be significant when operating based on the discharge. If the energy content is high, the error between modeled and realized production energy becomes significant when operated based on discharge.

In the studied river system unit *P5* has the lowest head of the plant and it is operated based on planned discharge. Operating based on discharge is chosen because deviations in discharge will cause considerable harm at water levels of downstream units and the error in produced energy is not significant. Unit *P6* automatically maintains a certain water level in the upper reservoir, so *P6* is operated based on arriving water flow. Units *P7* and *P8* are operated based on planned energy.

4.4 Planning and operation uncertainties

Uncertainties in the run-off forecasts and the difficulty of modeling the delay between units *P6* and *P7* are the main challenges in the planning and operation of the river system. The uncertainties have a substantial effect on the forecasting accuracy of the water levels. This uncertainty causes deviations from the original production plan.

The section of river between units *P6* and *P7* has many branches and riffles. These qualities of the river system are difficult to model and their behavior is unknown in different situations. Errors

in modeling the delay of the incoming water flow cause inaccuracy to the water level forecasts in situations when the water discharge is changed in the upper unit *P5*.

Inflow between units *P6* and *P7* is forecasted by Finnish Environmental Institute. The forecast is made for the 24-hour periods. This forecast resolution is not accurate enough to be used in the day-ahead production planning of the hydropower units. Especially sudden changes in the forecast need to be evaluated by the production planner. Sudden changes in the inflow are typically caused by torrential rain in the summer or snow melting in the spring. These type of changes in the weather are difficult to forecast. Also, modeling the effects of a heavy rain on the water flow of *IF1, IF2* and *IF3* have errors. Variations in the inflow which happen during the day cannot be seen in the 24-hour forecasts.

These difficulties in the planning of the production affect the operation of the river system. Uncertainty in the modeling of the delay between units *P6* and *P7* creates difficulties in calculating the natural inflow between the units. Total inflow to the unit can be calculated. The difficulty is to determine what the portion of the total inflow caused by the upper hydropower unit and what is the natural inflow.

Also, sudden changes in the weather in the summer can cause difficulties in the operation. *IF2* is a 147 km long river without dams to control the flow of the river. Torrential rain that hits the catchment area of the river causes a sudden and heavy rise in the inflow of *IF2*. These sudden changes are not easy to forecast. The route of the torrential rain is difficult to forecast and the changes in the inflow are challenging to model. The forecasted rise in the inflow is typically a day or two days off compared with the actual rise of the inflow. Changes in the inflow are seen when the water levels of *P7* does not act as forecasted.

The hydropower unit *P7* is a co-owned unit. The planning and operation of the plant are done by actor B acting as a service provider. The produced electricity is traded to the Nordic electricity market by the owners of the plant. The production is placed in the electricity balance of one of the unit's owners. This actor does not operate or plan the production of the unit. The production plans of units *P5*-*P8* is done every day before 10:30 a.m. This means that the production plans for the following day cannot be easily modified if the forecasted inputs change before the day-ahead market closes. All changes to the original production plans are sold or bought from the intraday market which has higher price uncertainty than the day-ahead market. Also, the flexible market-based fixing of the production plan is not easily possible because the changes to the production plans need to get approved by the market operator.

Hydropower units do not measure the flow through the turbine. The discharge of the hydropower unit is calculated using the hydroelectric power produced, the measured head of the plant and turbine efficiency curve. The head of the plant and hydroelectric power production are measured directly. The turbine efficiency curve is provided by the turbine manufacturer, which experimentally tests the efficiency of the turbine with different discharges. The total discharge of the plant may have errors if one or more of these measurements mentioned above is incorrect.

It was unknown if there are errors in the discharge measurements in the studied river system. Some concerns are caused by the difference between discharge measurements of the units *P5* and *P6*. This difference is presented in Figure 22 below.

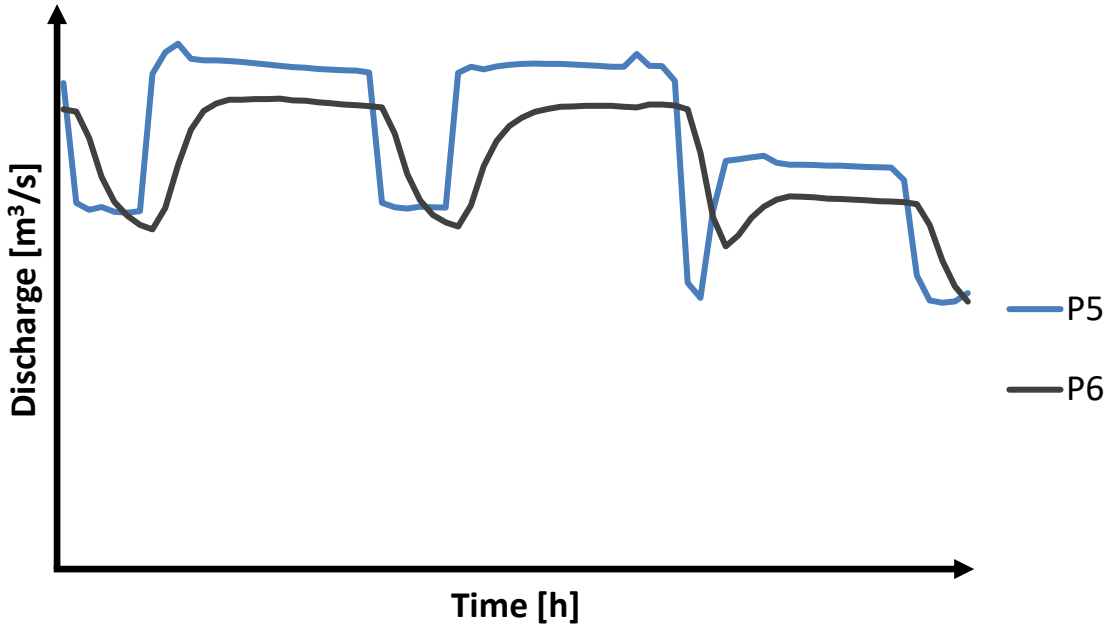

Figure 22. *Discharges of sequential units P5 and P6. There is no noticeable inflow between the plants.*

Unit *P6* is a typical RoR unit and its inflow is the discharge of unit *P5*. Unit *P6* has automation software that follows the incoming discharge from unit *P5*. Thus, the discharge of unit *P6* should be the same as unit *P5* after the delay of one or two hours. As can be seen from the figure above, there is a systematic error between the calculated discharges of units *P5* and *P6*. This error seems to be constant and can be caused by calculations in either unit.

4.5 Discharge measurement calibration

An outside company conducted flow measurements which were used to calibrate the discharge calculations. These tests were conducted for units *P5*, *P6*, and *P7* in September 2018. The flow was measured using Sontek RiverSurveyor M9 Acoustic Doppler Current Profiler (ADCP) attached to a remotely controlled Torrent Board V7. During these tests, the discharges of turbines were kept stable. Flow measurement was conducted vertically over the main stream of the river. Back and forth tests were done 5-7 times on average. The aim was to have the variation of individual measurements lower than 5 % and to measure over 50 % of the vertical length of the river. The average covariance of all tests was 3.2 %, which was well below the wanted level. The vertical length of the measurement was approximately 70 %, which was more than the target. Flow measurement calibrations were conducted for two turbines in unit *P5* and for two turbines in unit

P7. Unit *P7* has a total of three turbines, but one of the turbines was in revision during the calibrations.

The calibration measurements of turbines in unit *P5* were conducted in two lines below the plant. Test 4 was done somewhat further from the plant than the lower discharge tests 1-3. The higher discharges cause more turbulent flow which disrupts the measurement. Further away from the tail water these turbulent flows stabilize and measurement is possible. Unit *P5* was calibrated using four different discharge levels for both turbines. The calibration measures of turbine 1 are presented below in Figure 23.

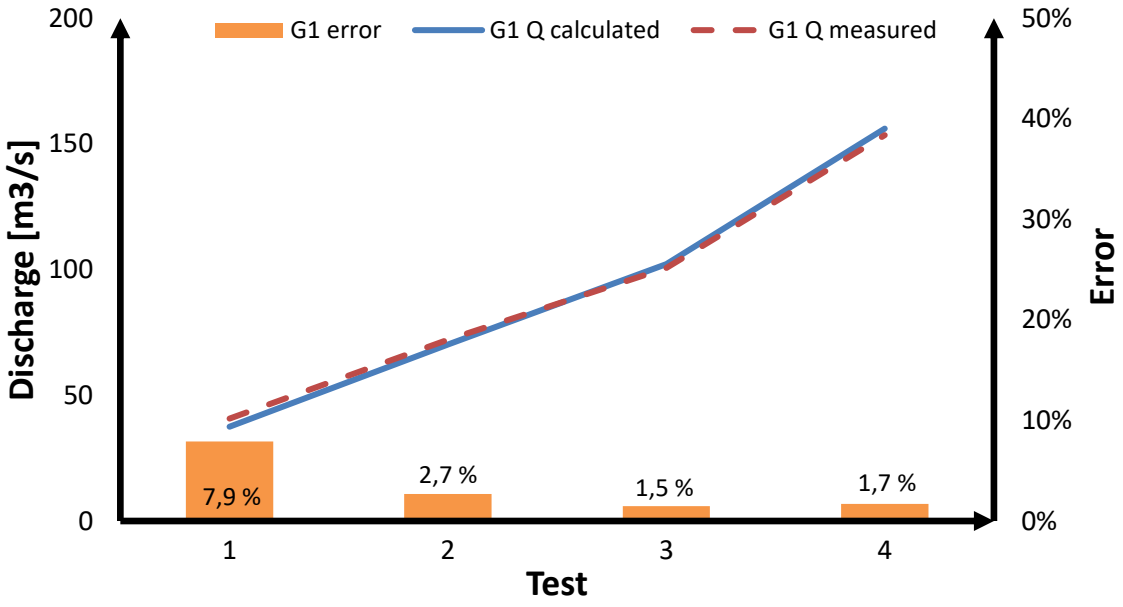

Figure 23. *Discharge calibration measurement of unit P5 turbine 1. The blue line presents the calculated discharge and the red dotted line illustrates measured discharge. Orange bars show the percentage error.*

As can be seen from Figure 23, the greatest relative errors between calculated and measured discharges are in the two lowest discharge tests. Percentual error emphasizes the difference between calculated and measured flows in low discharges. The highest difference is approximately 3 m^3/s in the 40 m^3/s test. Overall the measured and calculated discharges have a high correlation. Thus, no calibration is needed for the discharge calculation of the turbine. Below in Figure 24 is presented the measurements of turbine 2. The greatest errors are also at low discharge levels. Actual errors are relatively low and thus no calibration is needed.

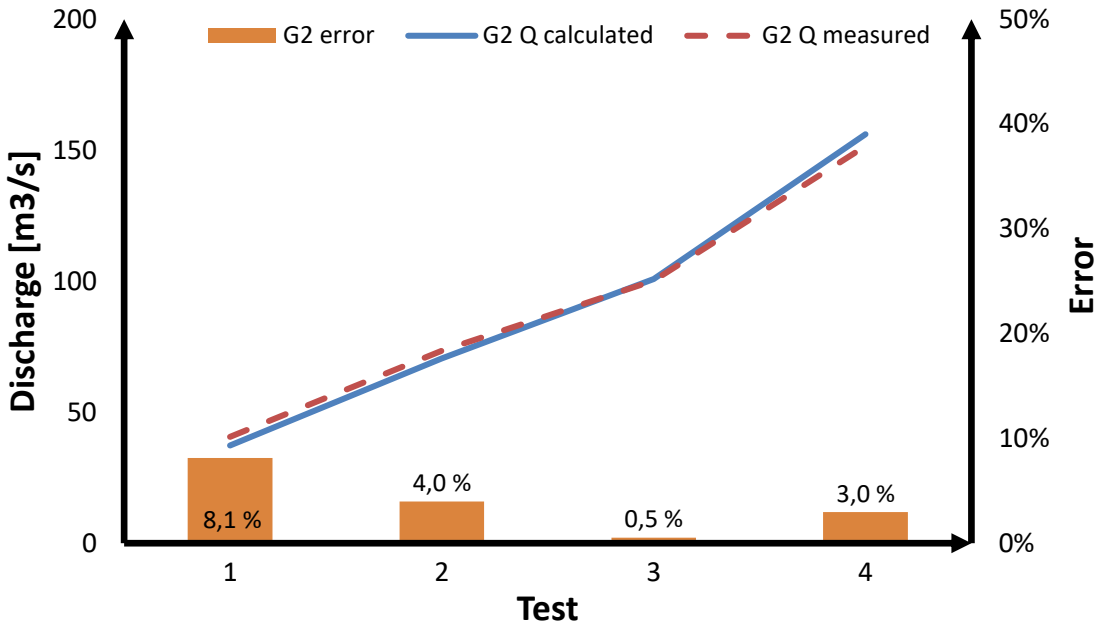

Figure 24. *Discharge calibration measurement of unit P5 turbine 2. The blue line presents the calculated discharge and the red dotted line illustrates measured discharge. Orange bars show the percentage error of each test.*

The calibration measurements of unit *P7* were conducted for two of the total three generators. The measurements were made also in two lines vertically across the river. The higher discharges test 5 was made also further downstream of the tail water than tests 1-4 because of the turbulent flows. The calibration measurements of unit *P7* turbine 1 is presented below in Figure 25.

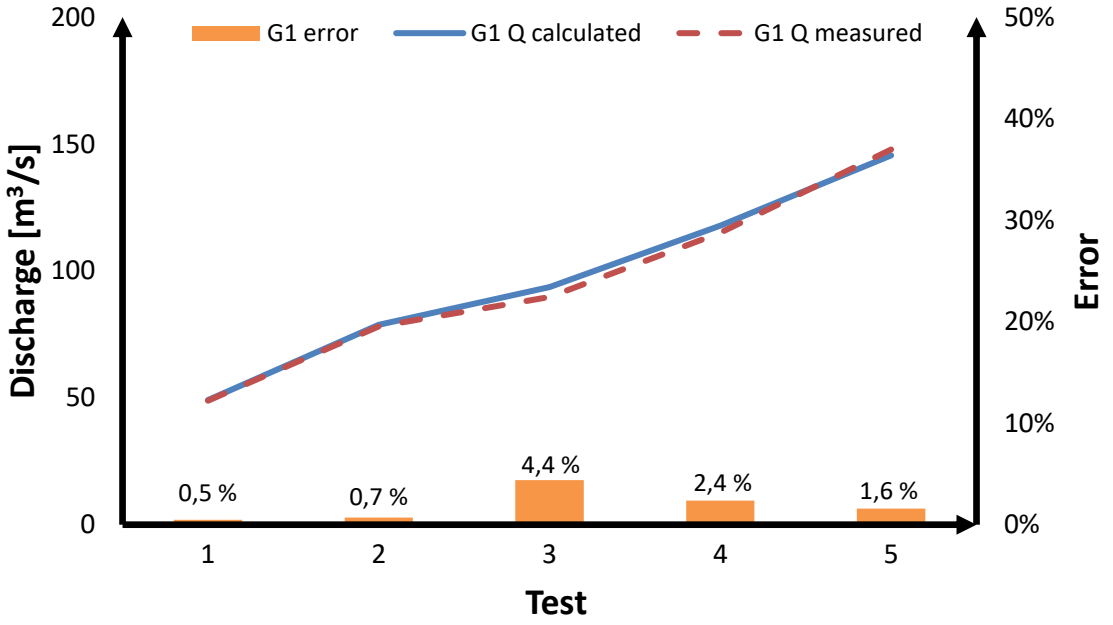

Figure 25. *Discharge calibration measurements of unit P7 turbine 1. The blue line presents the calculated discharge and the red dotted line illustrates measured discharge. Orange bars show the percentage error of each test.*

As can be seen from Figure 24, the measured and calculated discharges have a high correlation in all discharge levels. The highest differences can be seen in test 3, where the percentual difference is 4%. The actual difference is 4 $^{m^3}/_{s}$. The errors in all discharge levels are minor, thus no calibration to the calculation is needed.

The measurement results of turbine 3 are presented below in Figure 26. Actual errors are also relatively low and thus no calibration is needed.

Figure 26. *Discharge calibration measurements of unit P7 turbine 3. The blue line presents the calculated discharge and the red dotted line illustrates measured discharge. Orange bars show the percentage error of each test.*

Measurements were also conducted for unit *P6* to determine the possible leakage in the dam. First, the river flow was measured in the upper water. The second measurement was conducted in the downstream of the river. The separation of these measurements is 10 $^{m^3}/_{s}$. This indicates that the differences in discharges illustrated in Figure 22 are caused by a leakage in the unit *P6*.

4.6 Water flow meters

The meters are Workhorse Sentinel 600 kHz ADCP produced by Teledyne RD Instruments. The meters use Acoustic Doppler Current Profiler-technology to determine water flow. The measurement is based on the Doppler effect. The speed of the particles can be calculated from the frequency difference of the transmitted sound wave from the meter and the sound wave reflected from the particles of the water. The marketing material of Teledyne RD Instrument promises velocity accuracy to be 0.3 % of the water velocity and 50 meters of the measurement range (Teledyne RD Instruments, 2019). The water flow meters are mounted on the bottom of the river.

The meters have fixed AC-input and the measurement data is transferred via cable to a wireless transmitter.

The locations of the water flow meters *FM1* and *FM2* were presented in Figure 21. These locations were chosen because of the near proximity to the water level measurements *L1* and *L3*. The water level measurements are equipped with a firm AC connection thus no additional costs to electricity connections are required. In the chosen locations there is only one branch of river so all the water in the river system at that point can be measured with one meter. The water flow in *FM1* consists of the discharge of the unit *P6* and the inflows of *IF1* and *IF2*. The water flow meter *FM2* detects the discharge of *IF3* and the run-offs between *IF1 and IF2* in addition to the water flow in *FM1*.

The water flow meters were installed in December of 2017. Frazil ice detached the meter *IF2* in early January of 2018. Re-installation was possible a month later in February. The data transfer module broke down for a week in late January. There are no measurements available from either meter from that time period.

The water flow meters require calibration on different water flow levels to achieve accurate measurements. Hours before the test upper plants *P5* and *P6* were set to steady discharge. Calibration was done by measuring the accurate discharge with a mobile water flow meter and comparing the results with the installed flow meters. Any error between the measurements was fixed using a correction coefficient. Two of the three calibration tests were conducted in December of 2017. The last calibration was conducted in June 2018. The calibration levels were 100 m^3/s, 200 m^3/s and 500 m^3/s.

4.7 Data

The available data from the water levels and turbine discharges are saved in the energy management system. The present value is saved for a month in the system. The present value measurements can be used to calculate shorter average values than the hourly average measurement. History beyond that time is average value with a resolution of one hour.

The water flow meters measure the present value of the water flow. Twice in an hour, the present value is calculated into a half an hour average measurement of the flow. Twice an hour this averaged value is transferred into a server of a service provider. Once an hour the value is transferred from the server into the energy management system.

Relevant data measurements related to this thesis are the water level measurements *L1-L4*, the discharge measurements of hydropower units *P5-P7* and the measurements of the flow meters *FM1* and *FM2*.

The data used was transferred from the energy management system to Excel 2016. The analysis and the calculations were made performed using Excel 2016.

5. RESULTS AND DISCUSSION

5.1 Storing capacity test

Earlier research has studied the storing capacity factors and delays in the river system. These studies were conducted without the water flow measurement using only the water levels and the discharges of the hydropower units. The accurate storing capacity factor of *L4* is unknown despite the earlier research. A similar test as performed earlier was conducted with the water flow measurement.

The storing capacity test was performed in early February to form a clearer understanding of the phenomena in the river system. The principle of the test is to make changes in one hydropower unit at the time to isolate the phenomenon under review. The test was done with hydropower units *P5* and *P7* observing the water levels of *L1-L4* and the water flows of *FM1* and *FM2*. Hydropower unit *P6* was excluded from the test scheme. This decision was made because the plant is purely RoR unit thus it has no effect on the storing capacity tests.

The test started with a steady phase where the inflow between units *P5* and *P7* was determined. This was done by setting a steady 60 $^{m^3}/_{s}$ from unit *P5* for 10 hours before the beginning of the test. The reservoirs *L1-L4* between units *P5* and *P7* were close to their upper limits. Therefore, the arriving water flow to the upper reservoir of unit *P7* was confidently stabilized. At the end of the steady discharge phase, the inflow was defined by determining the discharge of unit *P7* when the water levels *L3* and *L4* remain constant. The inflow was 4 m^3/s at the beginning of the test.

60 m^3/s step-up in the discharge of the unit *P7* was done while the discharge of the unit *P5* was kept at the same 60 $^{m^3}/_{s}$. The discharge of the unit *P7* was approximately 140 $^{m^3}/_{s}$ during the emptying phase of the test. This phase continued for 15 hours. After the emptying phase, a step-down in the discharge of the unit *P7* was done. The inflow was determined again during the second steady phase. Inflow between units *P5* and *P7* had risen and was 10 $^{m^3}/_{s}$.

After the second steady phase, another step-up in the discharge of the unit *P5* was done. The increase in the discharge was 70 $^{m^3}/_{s}$. At the same time, the discharge of the unit *P7* was kept at a steady level of 70 $^{m^3}/_{s}$. The steady level consisted of the incoming discharge of unit *P5* and the inflow. The filling phase lasted for 23 hours. The data gathered from the test is presented in Figure 27 below.

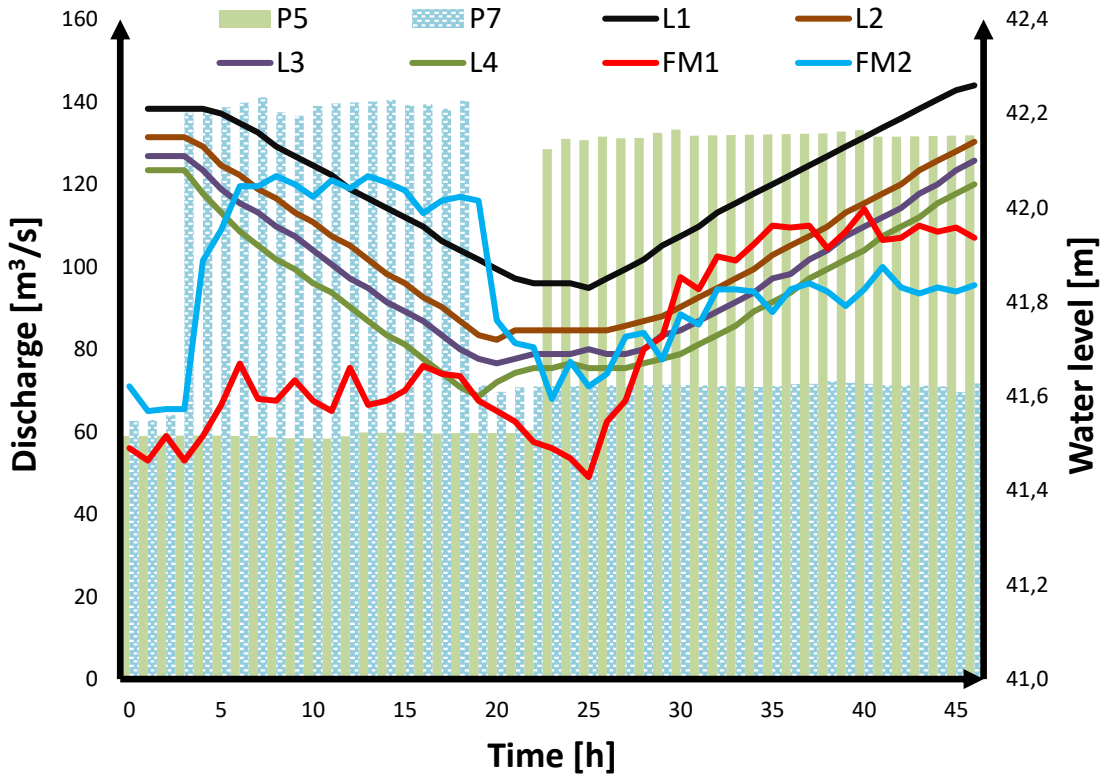

Figure 27. *The water levels and discharges during the water reservoir test. The red and green bars show the discharges of units P5 and P7. The red and blue lines are the water flow measurements of FM1 and FM2. The black, brown, purple and green lines are the water levels L1, L2, L3 and L4.*

The data from the discharges were gathered with the $^{m^3}/_{s}$ unit. The volume grows to very high numbers quickly if the calculations are done with SI-units. To overcome this problem an Hour Unit (*HU*) is used in the storing capacity factor calculations. One Hour Unit is the volume summed up by a discharge of 1 m³/s during an hour and is calculated as follows:

$$1\ HU = 1\ ^{m^3}/_{s} * \left(1\ h * \frac{3600\ s}{1\ h}\right) = 3600\ m^3. \tag{13}$$

The storing capacity factor (SCF) is used to describe how many cubic meters in seconds the difference between inflow and outflow should be so that it would cause a centimeter change in the water level of the reservoir. The storing capacity factor is calculated as follows:

$$SCF = \frac{\Delta q}{\Delta y}\frac{HU}{cm}. \tag{14}$$

The storing capacity factors were calculated for the water levels *L1*, *L3* and *L4*. The results are shown in Table 2.

Table 2. *The storing capacity factors of water levels L1, L2 and L4.*

	SCF emptying phase, $\left[\frac{HU}{cm}\right]$	*SCF filling phase,* $\left[\frac{HU}{cm}\right]$	*SCF average,* $\left[\frac{HU}{cm}\right]$
L1	34.0	32.4	33.2
L2	28.9	28.3	28.6
L4	28.0	28.4	28.2

The storing capacity can be determined from the emptying and the filling phase. The average values from the measurements are used in the future calculations in this thesis.

5.2 Analysis of the data from the water flow meters

A closer analysis of the data from the water flow meters was conducted. The available data was gathered during the regular operation of the river system. This analysis showed a clear oscillation in the data produced by the water flow meters. This oscillation is illustrated in Figure 28 below.

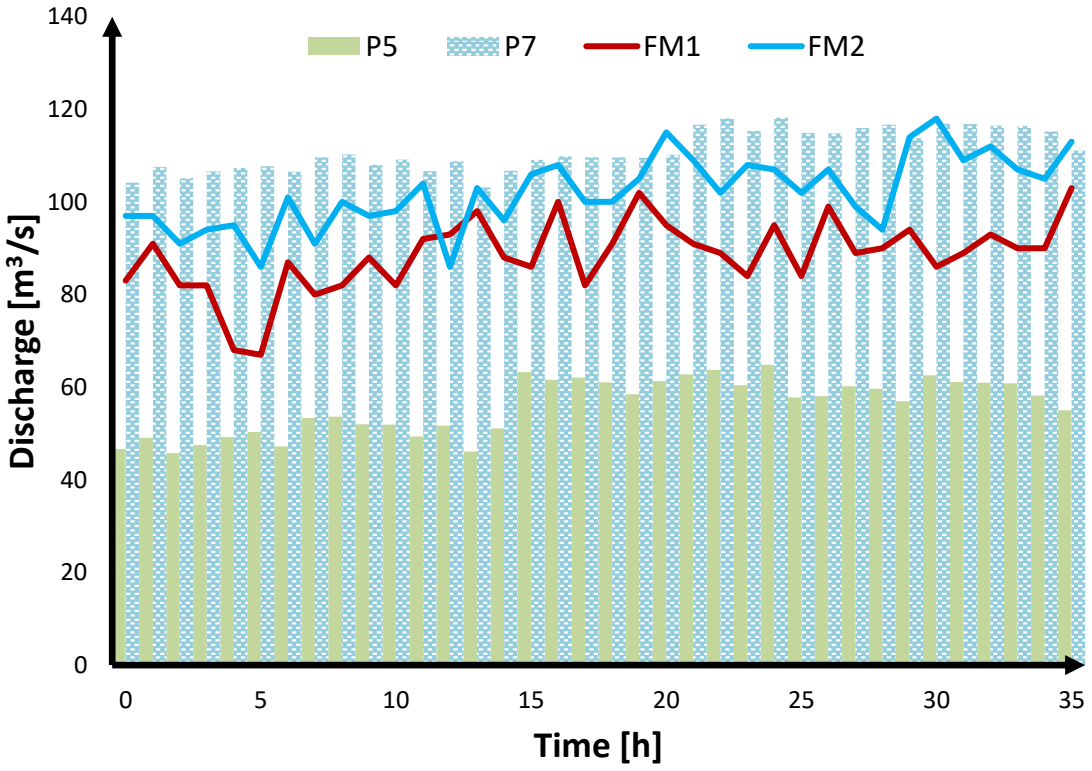

Figure 28. *The oscillation of the water flow meters during normal operation of the river system. The green and blue bars are the discharges of units P5 and P7. The red and blue lines are the water flow measurements of FM1 and FM2.*

The data in Figure 28 shows a typical situation in the river system. The discharge of unit *P5* was relatively low and the inflow between units *P5* and *P7* was approximately 55 $^{m^3}/_{s}$. The discharge of unit *P7* consisted of the inflow and the discharge of unit *P5* so the river was in balance. The measurements of the flow meters *FM1* and *FM2* are not stable even though the flow of the river is steady. The largest change between two consecutive measurements is 20 $^{m^3}/_{s}$ for both of the meters. The difference between the smallest and largest measure was 36 $^{m^3}/_{s}$ for *FM1* and 32 $^{m^3}/_{s}$ for *FM2*.

The experts in the company that installed the meters supposed that the oscillation is caused by local curling of water or other disturbances in the steady flow of the water. This explanation is not credible because the meters are installed in locations where the riverbed is smooth. A curling in a river system happens in rapids and in the tail water of a hydropower unit. Another, more plausible explanation for the oscillation is that the measurements are inaccurate.

During the analysis of the data, a clear correlation between the river flow and the height difference between water levels was found. The height difference increases during high discharges in the river. This clear correlation between the measurement of *FM1* and the height difference of water levels *L1* and *L3* is presented in Figure 29.

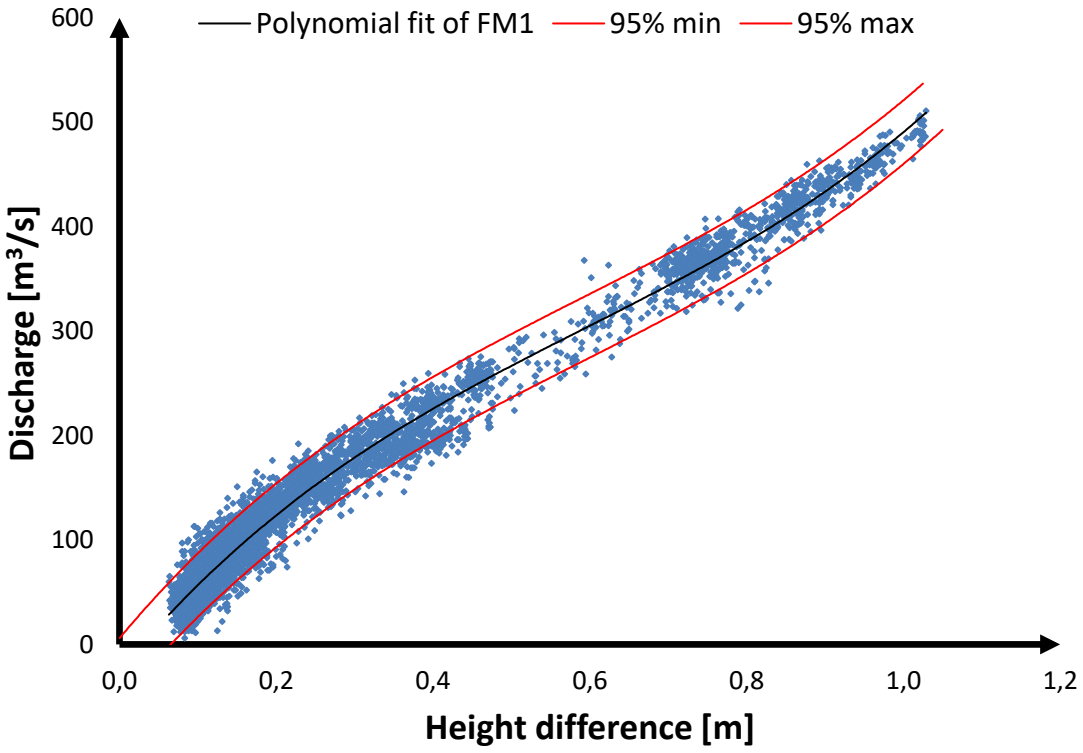

Figure 29. *The height difference between the water levels L1 and L3 as a function of the water flow FM1. The fit is a third-degree polynomial fit with an R^2-value of 0.9807. The standard error for the y-estimate is 15.24736. The red lines are the upper and lower limits of the 95% prediction band.*

The polynomial fit is created from the data available from the normal operation of the river. The area between the red prediction bands that are expected to enclose 95 % of the future data points. The prediction bands enclosed area include two types of uncertainties. The first is the uncertainty of the true position of the fit in relation to the data points. This uncertainty can be determined with the confidence band but is now included in the prediction band. The second uncertainty is the scatter of data around the fit. This uncertainty is mainly caused by the oscillation of the flow meters.

The relation between the height difference and the discharge measured by the flow meter can be seen from all the water level meters. The height difference between the water levels *L1* and *L3* was chosen because it has the best correlation to the discharge.

The correlation of the water flow measured by *FM2* and the height difference between the water levels *L3* and *L4* is presented in Figure 30.

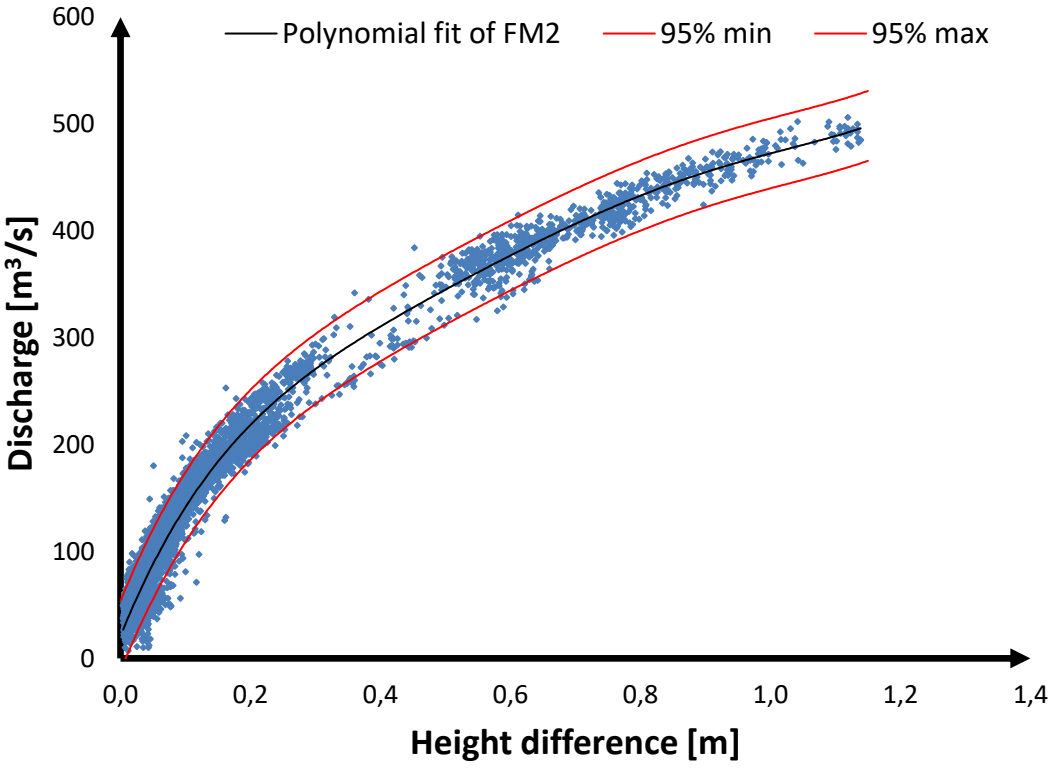

Figure 30. *The height difference between the water levels L3 and L4 as a function of the water flow FM2. The fit is a fifth-degree polynomial fit with an R^2-value of 0.9779. The standard error for the y-estimate is 16.68. The red lines are the upper and lower limits of the 95% prediction band.*

The standard error for the fit of *FM2* is only slightly larger than the standard error of *FM1.* Both standard errors of the fits are moderate. The enclosed area between the two red lines shown in the figure illustrates the 95% prediction band. The fifth-degree polynomial fit can be problematic: often there is an increased risk of overfitting when a high degree polynomial fits are used. Also, the high degree polynomial fit can illustrate the direction of the fit poorly when modeling phenomenon outside the training data set.

The fifth-degree polynomial fit was chosen because the lower degree polynomial fits correlate poorly with the training data. The behavior of the fit outside the training data is inaccurate. Discharges larger than 500 m^3/s are rare and typically happen only during heavy flooding. Modeling phenomena in a typical range of height differences is more important for the development of the operation and planning of the river system. Assuming that the future height differences will be in a typical range, the fifth-degree polynomial fit works reasonably. However, we should be aware that fifth-degree fit will most likely be unusable in extreme situations, e.g. if the height differences would grow much larger than the training data set suggests. Nevertheless, such situations are very rare in practice.

The measurement of the water flow meters can be calculated using the water level difference between the two chosen water levels. Figure 31 presents the calculated and the actual water flow measurement of *FM1* during a two-day time period.

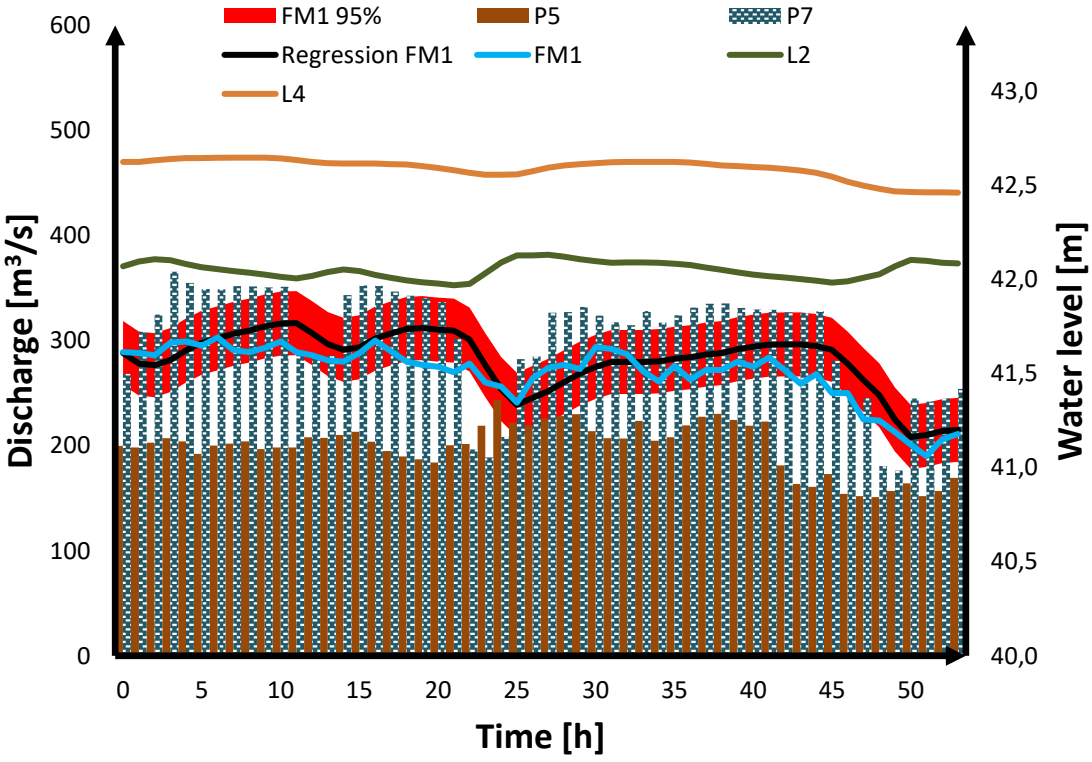

Figure 31. *A visualization of the water flow measurement calculated using the regression line. The calculated water flow of FM1 is marked as a black line. The red area presents the 95% prediction band. The light-blue is the actual measurement from the meter FM1. The green and the orange lines are the water level measurements used to calculate the height difference. The bars present the discharges of the units P5 and P7.*

The chosen data period is a quite typical situation in the river system. The hourly changes in the discharge of units *P5* and *P7* are clear. As can be seen from the figure, the calculated water flow correlates with the measured water flow. The measured water flow remains within the 95% prediction band apart from two short time periods where the measured water flow is lower. The calculated water flow does not have the oscillation seen in the actual water flow measurement. The

measurement of water level differences does not oscillate. This leads to steady results of calculated water flows when the steady measurement of water levels is used in the calculations. Figure 32 below illustrates the same results of the calculated and actual water flow of *FM2.*

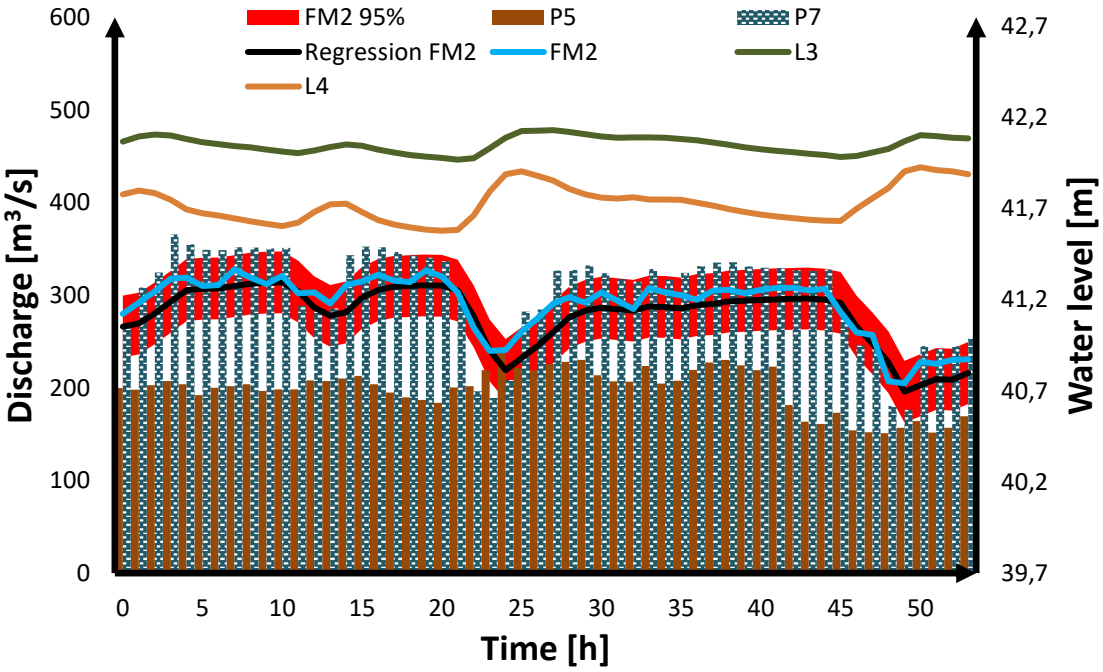

Figure 32. *A visualization of the water flow measurement calculated using the regression line. The calculated water flow of FM2 is marked as a black line. The red area presents the 95% prediction band. The light-blue is the actual measurement from the meter FM2. The green and the orange lines are the water level measurements used to calculate the height difference. The bars present the discharges of the units P5 and P7.*

The visualized data period is the same as in Figure 31. The calculated water flow of *FM2* always remains within the 95% prediction band. The calculated water flow measurement correlates well with the measured water flow of the meter. The calculated water flow correlates especially well with the measured water flow during times when considerable changes in the discharge of unit *P7* are made. The calculated water flow does not show the oscillation seen in the measurements of the meters.

5.3 The operating principle of the forecasting model

A new forecasting tool was created using the fits presented in the previous section. The water flow meters enabled us to observe the phenomena more closely between units *P5* and *P7*. The river section between units *P5* and *P7* has been modeled as one reservoir. The regression lines created enabled to divide the river section into three reservoirs and to model each section as its own reservoir. Figure 33 compares the previously used models with the one created in this thesis.

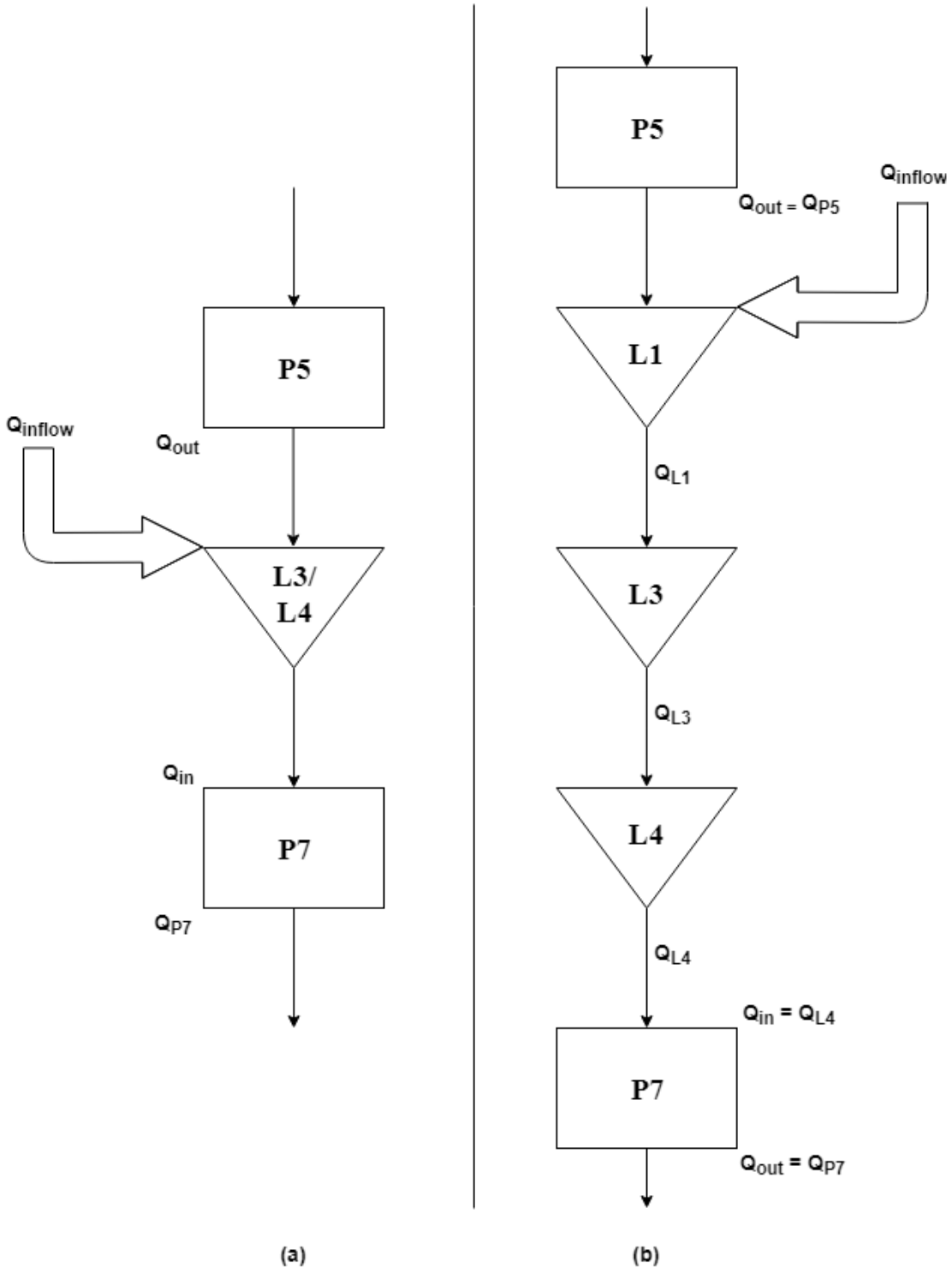

Figure 33. *The previously used modeling structure (a) compared to the one created in this thesis (b).*

The previously used model to forecast the water levels *L3* and *L4* uses the discharges of units *P5* and *P7,* the delay from *P5* to *P7* and the forecasted inflow. With this information, the incoming water is divided into time steps using the delay and the water level is forecasted using storing capacity factors for *L3* and *L4.*

The model created in this thesis uses the regression lines to determine the water flow in the three sections between units *P5* and *P7*. More detailed modeling of the river section makes it possible to understand the characteristics of each individual section. The first river section between unit *P6* and the water level *L1* is quite uncomplicated. Only distinctive features are the side streams *IF1* and *IF2*. Especially the inflow of the side stream *IF2* can burst rapidly. Forecasting rapid changes like this are difficult. The water flow in the river is divided into multiple branches in the second section between water levels *L1* and *L3*. The curving and branching shape of the river causes inaccuracy when determining the delays in different water flow levels. The second section has many rapids which can cause frazil ice in the winter. The inflow of the second section consists of the side stream *IF3* and the run-off. The distinctive feature of the third section between water levels *L3* and *L4* is the sharp turn in the riverbed. The sharp turn slows down the flow of the water causing an increasing height difference between the water levels *L3* and *L4,* especially in high discharges.

Dividing the portion of the river between the units *P5* and *P7* into three sections makes it easier to model the different features of the river sections. Analyzing the data from the intermediate stages enables better understanding than modeling the whole river section as one reservoir. The only controllable variables used in the forecasting calculations are the discharges of units *P5* and *P7*. The unit *P6* was left out of the calculations intentionally. The discharge of unit *P6* is not controllable because of the nature of the pure RoR unit. The minimal upper reservoir of unit *P6* cannot be used to regulate the power production of the river system. Thus, the production and the discharge of unit *P6* are dependent on the discharge of unit *P5*. The unit *P6* causes approximately an hour delay to changes made in the discharge of the unit *P5.* Also, the leakage of the unit *P6* has been tested only during one day in a steady discharge situation. It is unlikely that there are markable errors in the leakage measurements but the discharge of unit *P5* is more accurate.

The forecasted water levels are calculated with the hydro balance equations (7) and (9). The discharges of the first two reservoirs are calculated using the regression lines. The calculated discharge is used as the outflow from the reservoir. The outflow of the upper reservoir is the same as the inflow to the lower reservoir. The calculated discharges are used instead of the measured ones because the regression lines filter out the inconvenience oscillation of the meters. The measurements from the water flow meters are not required in the calculations.

The forecasted inflow between units *P5* and *P7* is to arrive fully at the section between the unit *P5* and the water level *L1*. This is a simplification and is not true in the reality. The portion to arrive in the first section of the whole inflow vary between 40-70% based on the initial calculations. The arriving portion to the first section increases when the total inflow increases. This happens because the total inflow consists of the side stream *IF2* to a greater extent. There were not enough accurate data to perform more accurate calculations to reliably divide the inflow to more realistic portions. The development of models often requires simplifications and some things needs to be left out of inspections. Figure 34 illustrates the forecasting calculation of the model.

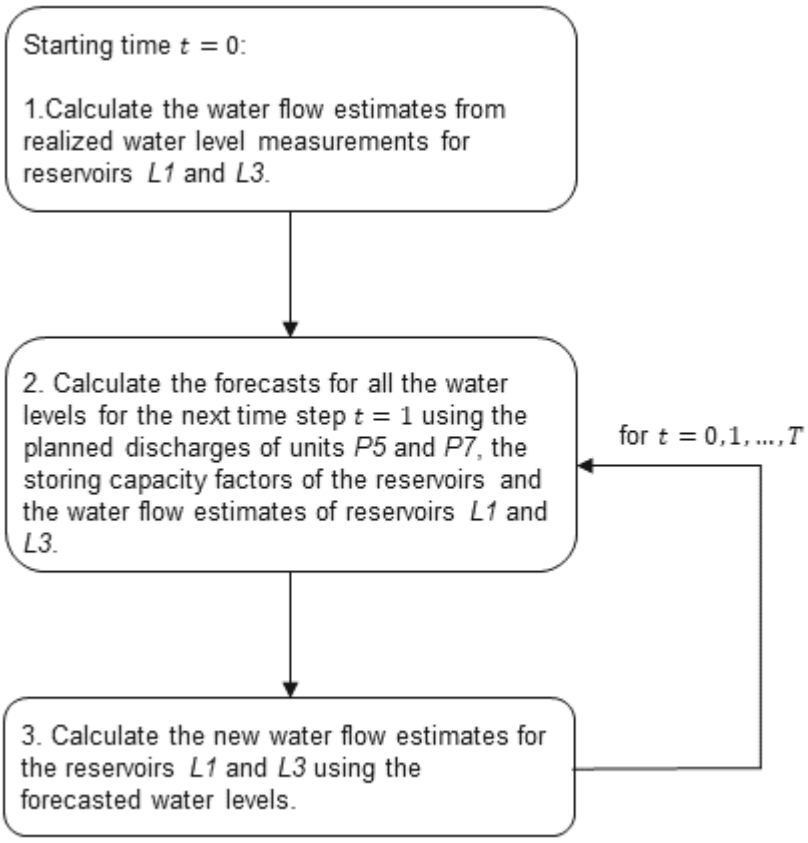

Figure 34. *The forecasting calculation of the model.*

The forecast is done once an hour with hourly resolution and the forecasting horizon is 24 hours. The calculation of the forecast starts at time step $t = 0$. In the first phase, the present water levels of *L1*, *L3* and *L4* at starting time step are used to calculate the discharges of reservoirs *L1* and *L3* using the regression lines. In the second phase, the forecasted inflow, the estimated delays between reservoirs and the planned discharges of units *P5* and *P7* are added to the calculations. With the addition information, all the incoming and outgoing water flows of all reservoirs are known. In the third-phase the water level forecasts of *L1*, *L3* and *L4* can be made for time step $t = 1$ using the storage capacity factors calculated in Table 2. The forecasted water levels of *L1, L3* and *L4* are used to calculate the forecasted discharges of the reservoirs. The phases two and three are repeated for all the time steps until the time horizon of 24 hours is forecasted.

The causes of error in the forecast were recognized during the development process of the forecasting tool. The most significant challenge in the calculation is that if the forecasted water levels are incorrect, they reflect directly to the forecasted discharges. An error in the forecasted discharge causes more error into the forecasted water levels. Thus, the errors in the forecasted water levels and the discharges of the reservoirs are cumulated during the forecasting horizon.

Other recognized sources of errors are the regression lines used to calculate the reservoir discharge from the water level differences, the storing capacity factors and the delays between different reservoirs. The standard error for the y-estimate for the reservoir *L1* is 15.24736 and 16.68 for the reservoir *L3*. This means that the actual discharge of the reservoir can be approximately 15 $m^3/_S$ greater or smaller than the calculated value. Using the storing capacity factors, the forecasted water level can be calculated to have approximately ±0.5 cm error on the first forecasted time step. The error does not directly cumulate, thus the error caused by the regression lines does not grow towards the end of the forecasting horizon. The storing capacity factors were determined on the basis of one test. To have more accurate knowledge of the actual storing capacity factors, more tests would be required. The forecasting inaccuracy caused by the error in the storing capacity factors does not directly cumulate over the forecasting horizon. The delays between the reservoirs also have error. The delay profiles are not exactly known. More water level measurements would be required to determine more accurate delay profiles between reservoirs. The error in the delay profiles does not cumulate during the forecasting horizon.

5.4 Model results

This section presents the forecasts calculated using the model presented in Figure 33b and 34. The data used in the calculation of the forecasts is actual data from the normal operation of the river system. The calculation requires the present water levels of *L1*, *L3* and *L4*, the planned discharges of the units *P5* and *P7* and the inflow. The forecast is then calculated for the water levels *L1*, *L3* and *L4* for 24 hours ahead. Figure 35 presents the forecast for water level *L1*.

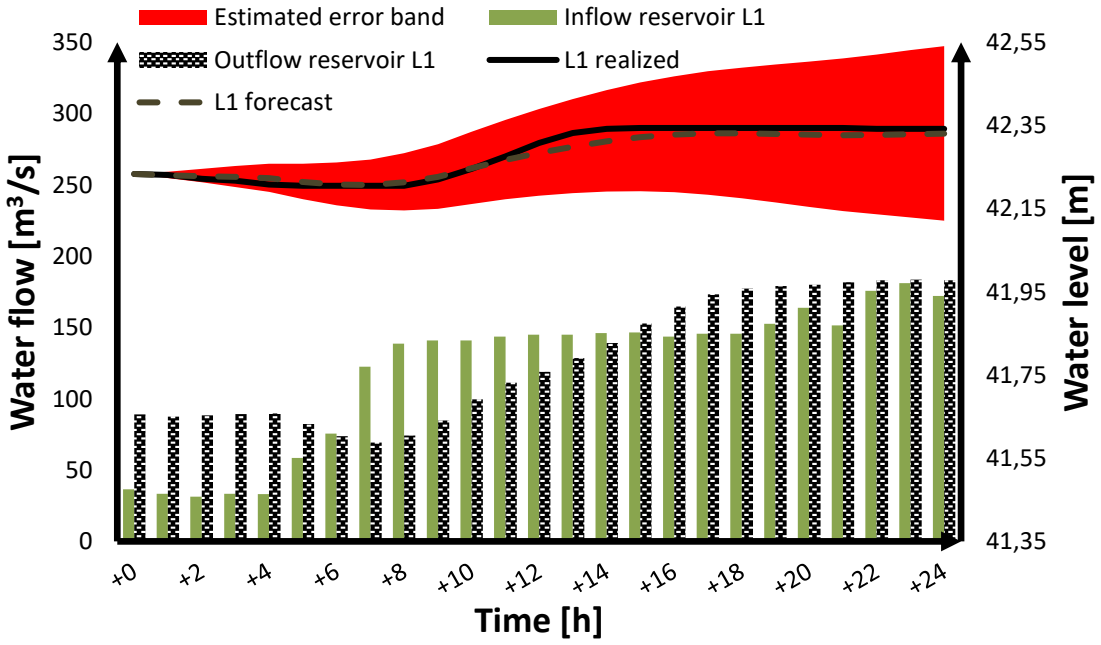

Figure 35. *The forecast for water level L1. The dotted line presents the forecasted water level and the black line is the realized value. The red area illustrates the estimated error band of the forecast. The green and purple bars are the inflow and outflow of the reservoir. The mean absolute error (MAE) of the forecast over the forecasting horizon is 0.0123 m.*

The estimated error band is calculated using the 95% prediction interval of the regression lines presented in Section 5.2. The prediction intervals can be calculated only using realized water levels. The estimated error band is based on the forecasted water levels, so it cannot be used as the prediction interval of the forecast. The limits of the estimated error band for the forecasted water levels are calculated with the presumption that the calculated water flow is on the upper or lower limit in every time step. The lower limit of the estimated error band is calculated using the lower limit of the prediction interval in all time steps. The upper limit of the estimated error band is calculated using the upper limit of the prediction interval.

The error band presents the uncertainty in the forecast caused by the error in the regression lines only. As can be seen from the figure, the error band becomes broader towards the end of the forecasting horizon. The error band is approximately 40 cm when forecasting values 24 hours ahead. Other sources of error would widen the error band even more. The error in the storing capacity factors or the delay profiles between reservoirs cannot be estimated reliably with the data available. Thus, the calculated error band can be described as an estimation, not the actual prediction interval of the forecast.

The forecasted and the realized values are in good agreement over the whole forecasting horizon. The SSE of the forecast is low and the forecast is accurate especially for the first 12 hours of the forecasting horizon. The forecasted change in the water level after the rise in the inflow to the reservoir is slower than the realized change in the water level. The forecasted water level ends up close to the realized water level after a couple of hours. Figure 36 presents the forecast for the water level *L3* during the same time period.

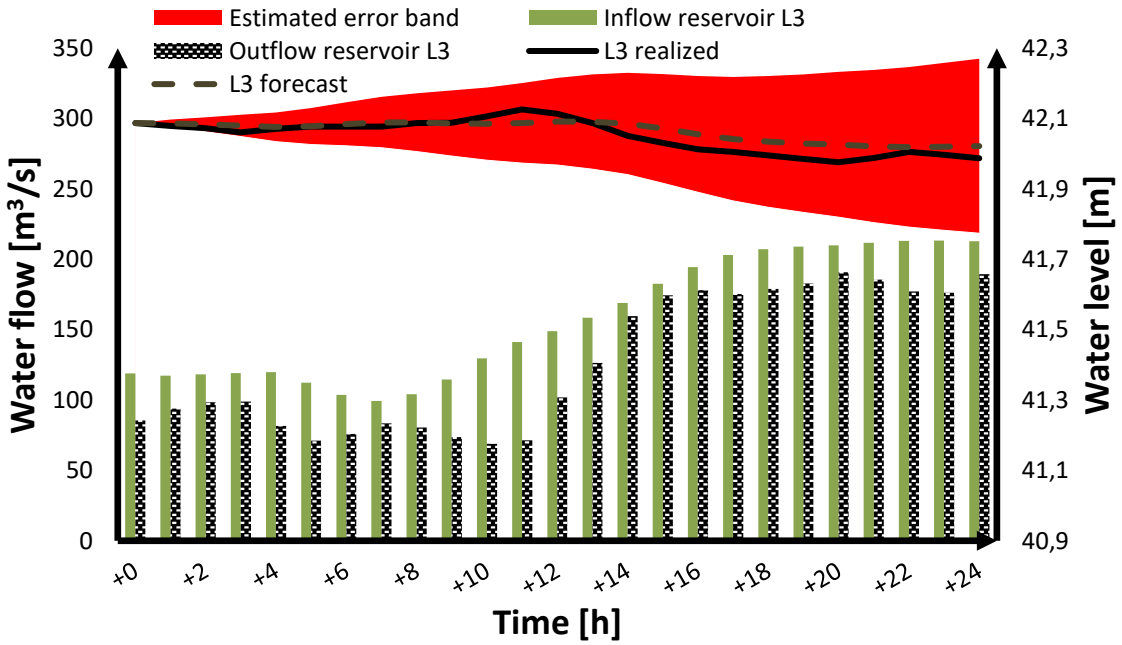

Figure 36. *The forecast for the water level L3. The dotted line presents the forecasted water level and the black line is the realized value. The red area illustrates the estimated error band of the forecast. The green and purple bars are the inflow and outflow of the reservoir. The MAE of the forecast is 0.0218 m.*

The estimated error band is approximately 50 cm at the end of the forecasting horizon and the SSE of the forecast is greater than the SSE of water level *L1*. The first 10 hours of the forecast follows the realized water level with good accuracy. The forecast reacts to the changes in the outflow slower than the realized water level causing error in the last 14 hours of the forecasting horizon. Figure 37 presents the forecast for the water level *L4* during the same time period.

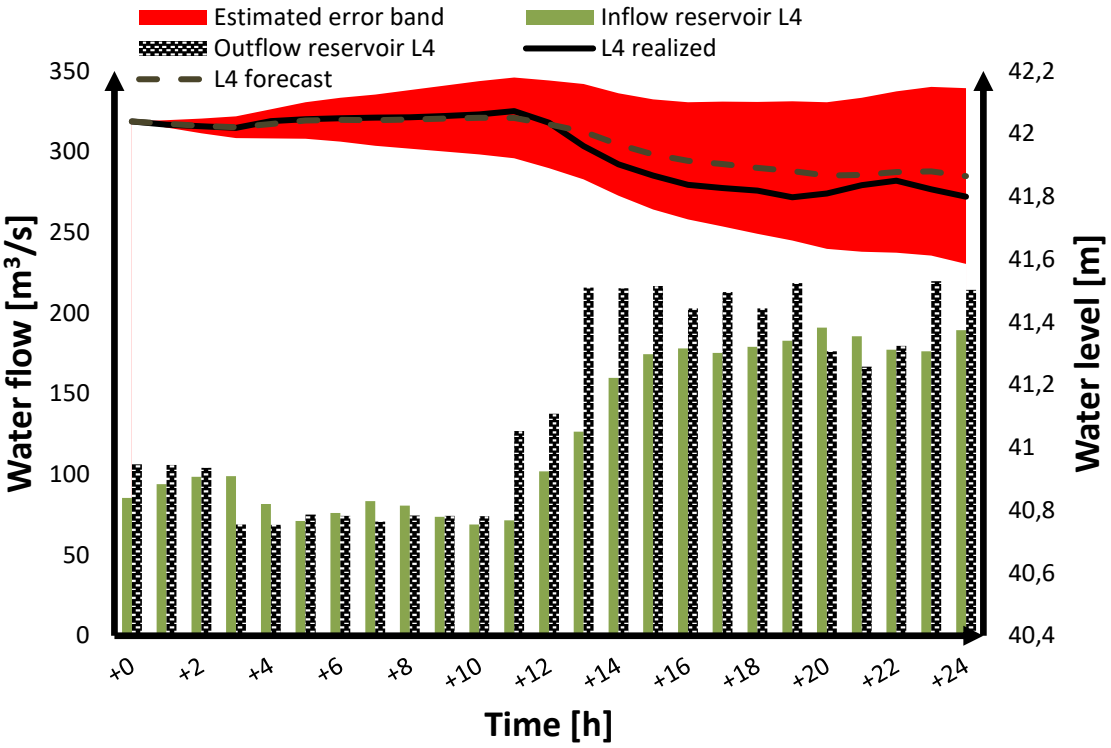

Figure 37. *The forecast for the water level L4. The dotted line presents the forecasted water level and the black line is the realized value. The red area illustrates the estimated error band of the forecast. The green and purple bars are the inflow and outflow of the reservoir. The MAE of the forecast is 0.0323 m.*

The forecast for the water level *L4* has the greatest SSE. This is caused by the error in the last 12 hours of the forecasting horizon. The forecast is good for the first 12 hours. The change in the outflow of the reservoir affects the water level more rapidly the forecast predicts. The highest actual error between forecasted and realized water level is approximately 7 cm.

The following figures present an example of a failed forecast. Figure 38 illustrates the forecasted water level of *L1*.

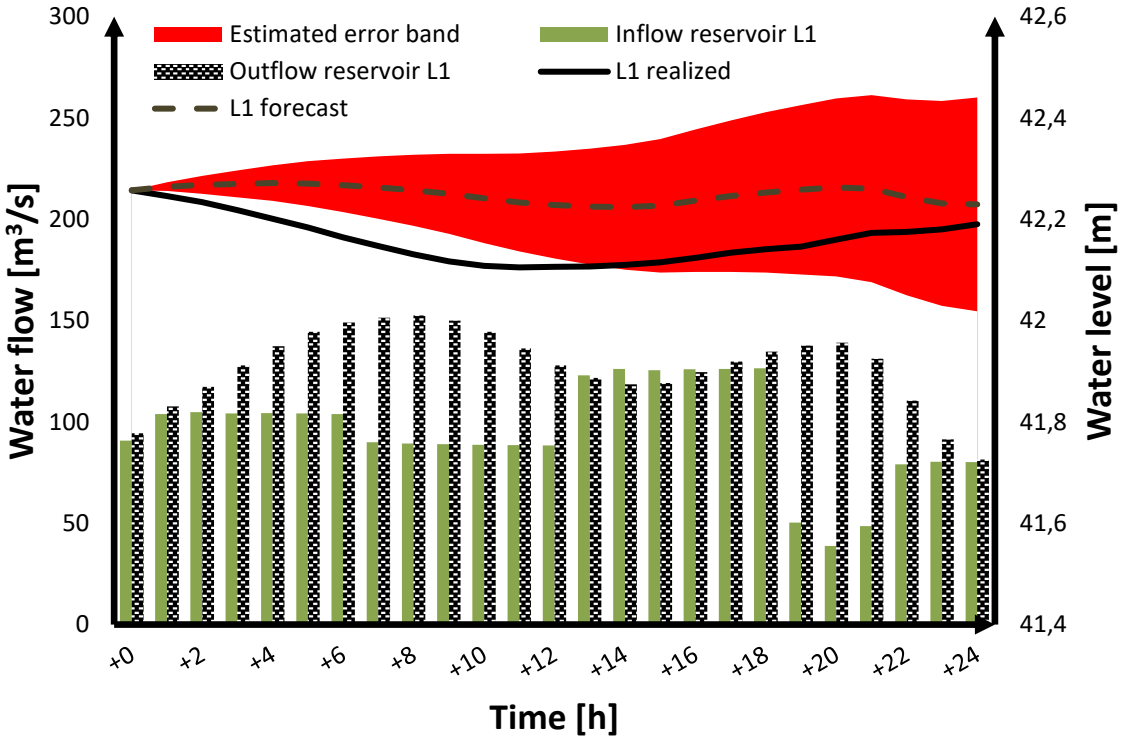

Figure 38. *A failed forecast for the water level L1. The dotted line presents the forecasted water level and the black line is the realized value. The red area illustrates the estimated error band of the forecast. The green and purple bars are the inflow and outflow of the reservoir. The MAE of the forecast is 0.0906 m.*

The forecasted water level has error from the first time step forward. The realized water level starts to decrease with a higher rate of change than the forecasted. The error reduces towards the end of the forecasting horizon. The forecasted water level is higher than the realized water level during the whole forecasting horizon resulting the model to overestimate the outflow of the reservoir *L1*. This illustrates the most important cause of error. The calculated outflow of the reservoir has an increasing error if the forecasted water level has error.

Figure 39 below presents the forecast for the water level *L3*. The error between forecasted and realized water levels starts to increase from the beginning of the forecast. The figure illustrates that the forecast has a slower rate of change than the realized water level has during changes in the inflow and outflow of the reservoir.

The error in the forecasted water level of *L3* is partially caused by the error in the calculated outflow of the upper reservoir *L1*. The outflow from reservoir *L1* is used directly as the inflow to reservoir *L3*. This means that the model calculates the incoming water flow to be greater than the actual inflow resulting the forecasted water level to have error. Towards the end of the forecasting horizon, the error between forecasted and realized water level of *L1* decreases resulting to a better forecast for water level *L3* in the end of the forecasting horizon shown in Figure 39. This does not change the fact, that the forecast for water level *L3* has markable error from the first time step onwards.

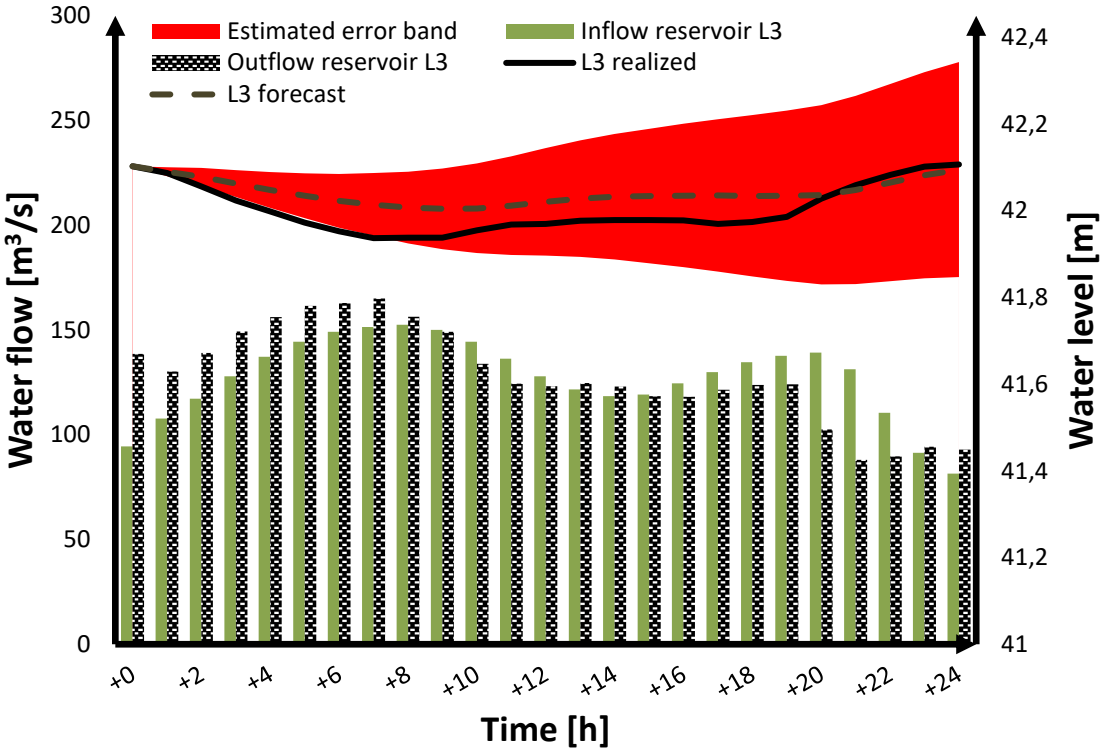

Figure 39. *A failed forecast of the water level L3. The dotted line presents the forecasted water level and the black line is the realized value. The red area illustrates the estimated error band of the forecast. The green and purple bars are the inflow and outflow of the reservoir. The MAE of the forecast is 0.04262 m.*

Figure 40 below presents the forecast for the water level *L4* during the same time period. The forecast of water level *L4* has the same characteristics as the forecasts of water levels *L1* and *L3*. The realized water level starts to decrease with a higher rate of change than the forecasted. The realized water level is outside of the estimated error band for the first 6 hours. This same phenomenon can be seen in all the forecasted water levels. As stated earlier, the actual prediction interval of the water level forecast includes more causes of error resulting the actual error band to be wider.

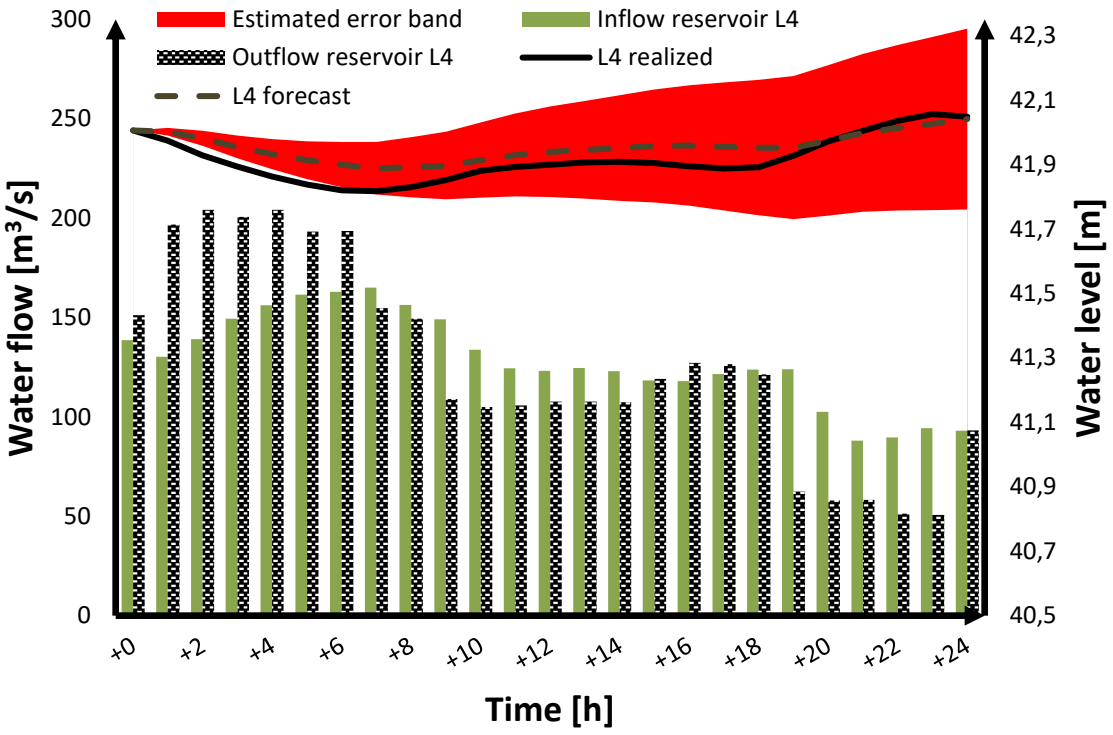

Figure 40. *A failed forecast of the water level L4. The dotted line presents the forecasted water level and the black line is the realized value. The red area illustrates the estimated error band of the forecast. The green and purple bars are the inflow and outflow of the reservoir. The MAE of the forecast is 0.0430 m.*

Error analysis was done by calculating MAE at time steps +6, +12, +18 and +24 from roughly 800 generated forecasts. The forecasts were calculated using data gathered from normal operation of the river system in 2017. The results are presented in Table 3 below.

Table 3. *MAE and max absolute errors of the forecasts.*

	Time step	Mean absolute error, [m]	Max absolute error, [m]
L1	6 h	0.0305	0.1218
	12 h	0.0452	0.1749
	18 h	0.0507	0.2163
	24 h	0.0515	0.2149
L3	6 h	0.0347	0.0383
	12 h	0.0428	0.2024
	18 h	0.0427	0.2128
	24 h	0.0393	0.2223
L4	6 h	0.0431	0.2337
	12 h	0.0485	0.2516
	18 h	0.0467	0.2576
	24 h	0.0448	0.2634

As can be seen in Table 3, MAE of the forecast increases towards the forecasting horizon. It is typically seen in forecasts that the accuracy decreases towards the forecasting horizon. Appendix A presents the distribution of the individual errors. All distributions resemble normal distribution.

Examination of the forecasted and realized water levels shows that the forecasted changes in the water levels are slower than the changes in the realized water levels. This phenomenon is seen during noticeable changes in the discharges of units *P5* and *P7*. The cause of this effect is most likely that the delays or the calculation of discharges from the water level differences does not react fast as required during the discharge changes of units *P5* and *P7*. The problem could be solved by conducting more thorough tests with different discharge changes. These tests would require more water level meters between the units. Modeling the storing capacity factors, the delay profiles between reservoirs and the how the water levels behave during discharge changes is possible with more accurate data.

Modelling the river section between units *P5* and *P7* with three separated reservoirs has many benefits when compared to the previous models used. Previous models determined the water level forecasts by calculating that certain amount of water released through unit *P5* arrives to unit *P7* with a certain delay. The approach created in this thesis aims at modeling the river section between units *P5* and *P7* as a difference equation system. The water flow out of a certain reservoir is modeled to be dependent on the slope of the water level, i.e. the height differences between water levels.

The main benefit of the new approach is that the change in the inflow between is seen as a change in the water level of *L1* resulting the change to be automatically added to the calculations. For example, in case when the inflow of *IF2* suddenly rises, the water level of *L1* rises causing the height difference between water levels *L1* and *L3* to increase. With higher height difference, the regression lines increase the water flow to the lower reservoirs without actions required from the user of the forecasting tool. This model is the first to study the behavior of water level *L1* and to create a model for forecasting the water level.

Determining accurate delay profile for the arriving water to unit *P7* after the release through unit *P5* has proved to be challenging previously. Modeling the long river section in shorter reservoirs allows more accurate modeling of delays between reservoirs. Determining delays in short distances has proved to be simpler than modeling delays in long distances. There is still room for progress in the more accurate modeling of the delays.

The regression lines introduced in Section 5.2 can be used to directly create economic benefit. The regression lines can be used to calculate the water flow in the river. The two water flow meters are no longer required to provide information. The economic benefits are gained by savings in the service fees for the company that installed the meters. The water flow data calculated using the regression lines has proven to be as accurate as the actual measurement from the meters. The calculated water flow does not include the disturbing oscillation that the measured water flow has.

The behavior of the forecasts in significantly high water level differences is a limitation of the results presented in this thesis. The calculation of water flows using the regression lines in remarkably high water level differences results in unreal values of water flow. This is caused by the behavior of the fifth-degree polynomial regression line of *FM2* outside the training data. This means in practice that the forecasting tool cannot be used in situations where the water level differences rise to high values because of frazil ice for example. Such situations happen rarely and forecasting water levels is not a priority during these complications.

6. CONCLUSION

This thesis studied the utilization of two water flow meters in a river system. The forecasting of water levels is essential in the operation and planning of hydropower. Forecasting tools with adequate accuracy enable the optimal market-based production of hydropower. However, modeling the physics in a river system is challenging because the dynamics of a river system are truly complex. Understanding the market-based operation of hydropower requires knowing of the electricity market. Different markets set the requirements which the production and operating of hydropower needs to fulfil. Understanding the dynamics of hydropower, such as water availability and production scheduling, creates opportunities as well as limitations to the production of hydropower. Each river system has its own limitations set by nature and the Governance Rule. Understanding these qualities sets the starting point of modeling the dynamics in a river system.

A clear objective for the results was set at the beginning of this thesis. The objective was to develop the near-future forecasting of the river section, especially the next 12 hours ahead. This research aimed to provide answers whether the water flow meters could improve the operation and planning of the river system and could the current forecasting tools be improved using the additional data available. In addition, the thesis tried to analyze how much time does the operator have to act when a relevant change in the inflow is noticed.

Data acquired from the meters allowed to find a correlation between the height difference of the water levels and the water flow of the river. The correlation was presented as a regression line which can be used to calculate the water flow in the river system. The correlation between the height difference and the water flow was noticed between all height differences and measured water flow. The chosen regression lines have the best correlation with the data.

A new forecasting model was created using the regression lines. In the forecasting model a section of the river is divided into three separate reservoirs in the forecasting model. The modeling of the river section in multiple reservoirs enables more accurate modeling of the various characteristics of the sections.

The new forecasting tool should be considered as a concept that could be developed further, rather than something that could be taken into operative use straight away. The number of times when the error is large between the forecast and realized water level is too high. The error distribution needs to be narrower before the forecasting tool could be taken into operative use.

Real-time monitoring of the water flow alone does not produce value when considering the cost of the measurement. Measurement must be used to make observations of the phenomena in a river system. This aids at developing the models that create value, not just passively observe the flow of the river.

Adding the real-time water flow measurement of the meters to the previously created forecasting tools does not improve the forecasting accuracy. The results suggest that improving the accuracy with water flow measurement in an open river channel requires the river section to be modeled in multiple reservoirs. Even after that, more water level data is required to improve the accuracy of the model created in this thesis in order to outperform the previous models.

The studies of the water flow measurement did not provide any further information on how much time the operator has to act when a relevant change in the runoff is noticed. To study the topic more carefully, economic investments are required to conduct tests using the tracer method to determine the delays to the unit *P7*. The water flow measurement did not prove to be useful in order to determine the delay profiles during the storing capacity test introduced in Section 5.1. More comprehensive water level measurement should be more useful when defining the water delay profiles.

Achieving the same accuracy that has been gained studying the river section with step-response tests and modeling it as one reservoir has proven to be difficult with the available data. The accuracy achieved in this thesis is as good as possible with four water level measurements between the units *P5* and *P7*. However, the model can be used to further develop the forecasting tool to accomplish the objective. The results of this thesis introduce the development trend for which the development of forecasting models of this river system could be developed.

A forecasting tool with better accuracy can be achieved with economic investments. There are cost-effective temporary water level meters available in the market. The meters measure the water level with a pressure sensor or an ultrasonic sensor and they include an own battery. These meters could be attached to stationary structures along the river section. Approximately ten meters would provide more data enabling the accuracy to be developed more. The key point in the development is to model the long river section with more than three reservoirs.

More research is also required to determine the portions of the total inflow that arrives to different reservoirs. Individual water level forecasts can be improved with more accurate information regarding the inflow. The inflow is modeled so that it arrives fully to reservoir *L1* which is a simplification. An outside company could be utilized to determine how the total inflow consist of the runoff and the inflows *IF1* - *IF3.* With more accurate information of the portions of the inflow that arrives to a specific reservoir would probably improve the forecasting accuracy.

All in all, this thesis suggests that no more water flow measurements are needed in the future. The meters have produced data for almost one and a half years, which is enough data for future modelling purposes and new data does not seem to add value anymore. Instead, this thesis suggests that more data about the water level is needed in order to develop a better model for the forecasting. This could be achieved e.g. by acquiring a water level meter as discussed above.

REFERENCES

Alnæs, E. N., Grøndahl, R. B., Fleten, S-E., Boomsma, T. K. (2015). Insights from Actual Day-Ahead Bidding of Hydropower, International Journal of Sustainable Energy Planning and Management, Vol. 07, pp. 37–58. DOI: 10.5278/ijsepm.2015.7.4.

Antila, H. (1997). Hydro Power Dynamics in Power System Planning, Tampere University of Technology, 128p.

Bai, Y., Chen, Z., Xie, J., Li, C. (2016). Daily reservoir inflow forecasting using multiscale deep feature learning with hybrid models, Journal of Hydrology, Vol. 532, pp. 193-206. DOI: 10.1016/j.jhydrol.2015.11.011.

Bellman, R., Dreyfus, S. (1966). Applied Dynamic Programming, Princeton U. P., 363 p.

Catalão, J. P. S., Mariano, S. J. P.S., Mendes, V. M. F., Ferreira, L. A. F. M. (2007). Profit-Based Short-Term Hydro Scheduling considering Head-Dependent Power Generation, IEEE PowerTech, pp. 1362–1367.

Catalão, J. P. S., Mariano, S. J. P.S., Mendes, V. M. F., Ferreira, L. A. F. M. (2006). Parameterisation effect on the behaviour of a head-dependent hydro chain using a nonlinear model, Electric Power Systems Research, Vol. 76, pp. 404–412. DOI: 10.1016/j.epsr.2005.09.002.

Crona, M. (2012). Evaluation of Flexibility in Hydropower Stations. Uppsala Universitet. Available at: http://www.diva-portal.org/smash/get/diva2:495430/FULLTEXT02.pdf (Accessed: 28 January 2019).

Dasgupta, S. (2006) Algorithms. McGraw-Hill, 336 p.

Dixon, S. L. and Hall, C. (2013) Fluid Mechanics and Thermodynamics of Turbomachinery: Seventh Edition. DOI: 10.1016/C2011-0-05059-7.

Energiateollisuus (2017). Energiavuosi 2016. Available at: https://energia.fi/ajankohtaista_ja_materiaalipankki/materiaalipankki/energiavuosi_2016_sahko_sahkonkaytto_kaantyi_nousuun.html (Accessed: 28 January 2019).

Energiateollisuus (2019a). Energiavuosi 2018 - Sähkö. Available at: https://energia.fi/files/1407/Energiavuosi_2018_Sahko.pptx (Accessed: 14 January 2019).

Energiateollisuus (2019b). Vesivoima. Available at: https://energia.fi/perustietoa_energia-alasta/energiantuotanto/sahkontuotanto/vesivoima (Accessed: 28 January 2019).

Energy Storage News (2017). EnergyAustralia ponders world's largest seawater pumped hydro energy storage plant. Available at: https://www.energy-storage.news/news/energyaustralia-ponders-worlds-largest-seawater-pumped-hydro-energy-storage (Accessed: 5 February 2019).

Entsoe (2017). Supporting Document on Technical Requirements for Frequency Containment Reserve Provision in the Nordic Synchronous Area, p. 25. Available at: https://energinet.dk/-/media/Energinet/El-RGD/El-PBU/Dokumenter/FCR-Dokumenter/Supporting-Document-on-Technical-Requirements-for-Frequency-Containment-Reserve-Provision-in-the-Nor.pdf (Accessed: 28 January 2049).

Eurelectric (2011). Hydro in Europe: Powering Renewables. Available at: https://www3.eurelectric.org/media/26690/hydro_report_final-2011-160-0011-01-e.pdf (Accessed: 5 February 2019).

Fingrid (2018). Reserve products and reserve market places. Available at: https://www.fingrid.fi/globalassets/dokumentit/en/electricity-market/reserves/reserve-products-and-reserve-market-places.pdf (Accessed: 24 January 2019).

Fingrid (2019a) Frequency Containment Reserves. Available at: https://www.fingrid.fi/en/electricity-market/reserves_and_balancing/frequency-containment-reserves/ (Accessed: 2 January 2019).

Fingrid (2019b). Integrity of price areas. Available at: https://www.fingrid.fi/en/electricity-market/market-integration/integrity-of-price-areas/ (Accessed: 24 January 2019).

Fingrid (2019c). Reserves and balancing power. Available at: https://www.fingrid.fi/en/electricity-market/reserves_and_balancing/#reserve-products (Accessed: 24 January 2019).

Finnish Environment Institute (2019a). Tarkka. Available at: http://syke.fi/tarkka (Accessed: 26 February 2019).

Finnish Environment Institute (2019b). Watercourse regulation. Available at: https://www.ymparisto.fi/en-US/Waters/Use_of_water_resources/Watercourse_regulation (Accessed: 6 February 2019).

Finnish Environment Institute (2019c). Watershed simulation and forecasting system - brochure. Available at: http://www.syke.fi/download/noname/%7B46044A4B-F779-43E5-8B80-E2501DF98A45%7D/91524 (Accessed: 6 February 2019).

Flatabo, N., Doorman, G., Grande, Randen, H., Wangensteen, I. (2003). Experience with the Nord Pool design and implementation, IEEE Transactions on Power Systems, Vol. 18(2), pp. 541–547. DOI: 10.1109/TPWRS.2003.810694.

Førsund, F. R. (2007) Hydropower Economics. Springer. Available at: https://link-springer-com.libproxy.tut.fi/content/pdf/10.1007%2F978-0-387-73027-1.pdf (Accessed: 29 January 2019).

Fosso, O. B., Gjelsvik, A., Haugstad, A., Mo, B., Wangensteen, I. (1999). Generation scheduling in a deregulated system. The Norwegian case, IEE Transaction on Power Systems, Vol. 14, pp. 75–81.

Furnans, J., Austin, B. (2007). Hydrographic survey methods for determining reservoir volume, Environmental Modelling & Software, Vol. 23, pp. 139-146. DOI: 10.1016/j.envsoft.2007.05.011.

Ghosh, S. N., Desai, V. R. (2006). Environmental Hydrology and Hydraulics: Eco- Tehnological Practices for Sustainable Development. Science Publishers.

IEA-ETSAP (2015). Hydropower Technology Brief. Available at: https://www.irena.org/Document-Downloads/Publications/IRENA-ETSAP_Tech_Brief_E06_Hydropower.pdf (Accessed: 28 January 2019).

IEA (2018). Key World Energy Statistics 2018. Available at: https://webstore.iea.org/download/direct/2291?filename=key_world_2018.pdf (Accessed: 28 January 2019).

IRENA (2012). Renewable Energy Cost Analysis - Hydropower. Available at: https://www.irena.org/-/media/Files/IRENA/Agency/Publication/2012/RE_Technologies_Cost_Analysis-HYDROPOWER.pdf (Accessed: 25 January 2019).

IRENA (2018). Renewable Power Generation Costs in 2017. Available at: https://www.irena.org/-/media/Files/IRENA/Agency/Publication/2018/Jan/IRENA_2017_Power_Costs_2018.pdf (Accessed: 25 January 2019).

Kervinen, T. (2010). A linear programming approach to estimate hydropower supply in the Nordic electricity market. Aalto University. Available at: https://pdfs.semanticscholar.org/b0eb/90d64439b8fe49b991884a5ea13979aca8d4.pdf (Accessed: 20 February 2019).

Kinnunen, M. (2013). Short-term planning of hydropower in a co-owned river system. Aalto University.

Kongelf, H., Overrein, K. (2017). Coordinated Multimarket Bidding for a Hydropower Producer using Stochastic Programming. Norwegian University of Science and Technology. Available at: https://brage.bibsys.no/xmlui/bitstream/handle/11250/2469855/17162_FULLTEXT.pdf?sequence=1&isAllowed=y (Accessed: 19 February 2019).

Labadie, J. W. (2004). Optimal Operation of Multireservoir Systems: State-of-the-Art Review, Journal of Water Resources Planning and Management, Vol. 130(2), pp. 93–111. DOI: 10.1061/(asce)0733-9496(2004)130:2(93).

Lummikko, R. (2017). Development of water system models with step-response tests. Tampere University of Technology. Available at: https://dspace.cc.tut.fi/dpub/bitstream/handle/123456789/24675/Lummikko.pdf?sequence=1 (Accessed: 15 January 2019).

Mäkiharju, J. (2012). The Development and Calibration of a Mid-Term Planning Model of a Co-Owned Hydropower System. Tampere University of Technology.

Nasdaq Commodities (2019). Nordic Power Products. Available at: https://business.nasdaq.com/trade/commodities/products/power-derivatives/nordic.html (Accessed: 22 January 2019).

Nord Pool (2017). Annual Report 2017. Available at: https://www.nordpoolgroup.com/globalassets/download-center/annual-report/annual-report-nord-pool_2017.pdf (Accessed: 23 January 2019).

Nord Pool (2018). The Nordic Electricity Exchange and The Nordic Model for a Liberalized Electricity Market. Available at: https://www.nordpoolgroup.com/globalassets/download-center/rules-and-regulations/the-nordic-electricity-exchange-and-the-nordic-model-for-a-liberalized-electricity-market.pdf (Accessed: 28 December 2018).

Nord Pool (2019a). Bidding areas. Available at: https://www.nordpoolgroup.com/the-power-market/Bidding-areas/ (Accessed: 22 January 2019).

Nord Pool (2019b). Day-ahead market. Available at: https://www.nordpoolgroup.com/the-power-market/Day-ahead-market/ (Accessed: 15 January 2019).

Nord Pool (2019c). History. Available at: https://www.nordpoolgroup.com/About-us/History/ (Accessed: 2 January 2019).

Nord Pool (2019d). Market data. Available at: https://www.nordpoolgroup.com/Market-data1/#/nordic/map (Accessed: 2 January 2019).

Nord Pool (2019e). Price calculation. Available at: https://www.nordpoolgroup.com/trading/Day-ahead-trading/Price-calculation/ (Accessed: 2 January 2019).

Nord Pool (2019f). The power market. Available at: https://www.nordpoolgroup.com/the-power-market (Accessed: 2 January 2019).

Nordic Energy Regulators (2014). Nordic Market Report 2014 Development in the Nordic Electricity Market. Available at: http://www.nordicenergyregulators.org/wp-content/uploads/2014/06/Nordic-Market-Report-2014.pdf (Accessed: 14 January 2019).

Ødegård, H. L., Eidsvik, J., Fleten, S.-E. (2019). Value of information analysis of snow measurements for the scheduling of hydropower production, Energy Systems. Springer Berlin Heidelberg, Vol. 10(1), pp. 1–19. DOI: 10.1007/s12667-017-0267-3.

Paasonen-Kivekäs, M., Peltomaa, R., Vakkilainen, P., Äijö, H. (2016). Maan vesi- ja ravinnetalous. Salaojayhdistys ry, Available at: http://salaojayhdistys.fi/wp-content/uploads/2016/05/web_maanvesijaravinnetalous_B5_2016.pdf (Accessed: 25 January 2019).

Pelkola, L. (2018). Decision Support System for Hydropower Planning under Inflow Uncertainty. Aalto University. Available at: https://aaltodoc.aalto.fi/handle/123456789/32392 (Accessed: 15 January 2019).

Pogosjan, D., Winber, J. (2013). Förändringar av marknadsdesign och deras påverkan på balanshållningen i det svenska kraftsystemet. Uppsala Universitet.

Scharff, R., Egerer, J., Söder, L. (2014). A description of the operative decision-making process of a power generating company on the Nordic electricity market, Energy Syst, Vol. 5, pp. 349–369. DOI: 10.1007/s12667-013-0104-2.

Scharff, R., Amelin, M. (2015). Trading behaviour on the continuous intraday market Elbas, Energy Policy, Vol. 88, pp. 544–557. DOI: 10.1016/j.enpol.2015.10.045.

Singh, V. K., Singal, S. K. (2017). Operation of hydro power plants-a review, Renewable and Sustainable Energy Reviews, Elsevier, Vol. 69, pp. 610–619. DOI: 10.1016/j.rser.2016.11.169.

Skjelbred, H. I., Kong, J. (2018). Operational hydropower simulation in cascaded river systems for intraday re-planning, 20th Power Systems Computation Conference, PSCC 2018. Power Systems Computation Conference, pp. 1–7. DOI: 10.23919/PSCC.2018.8442510.

Snyman, J. (2005). Practical Mathematical Optimization, Springer, Boston, MA. DOI: https://doi-org.libproxy.tut.fi/10.1007/b105200

Souza, T. M., Diniz, A. L. (2012). An accurate representation of water delay times for cascaded reservoirs in hydro scheduling problems, IEEE Power and Energy Society General Meeting. IEEE, pp. 1–7. DOI: 10.1109/PESGM.2012.6344655.

Teledyne RD Instruments (2013). Datasheet, p. 2. Available at: http://www.teledynemarine.com/Lists/Downloads/sentinel_datasheet_lr.pdf (Accessed 05 January 2019).

Tuovinen, M. (2019). Takingover of a River System with Hydro Assets. Tampere University of Technology.

UPM Energy Oy (2019). The Governance Rule. Confidential information.

Vattenfall (2019). Vesivoima - toimintaperiaate. Available at: https://corporate.vattenfall.fi/tietoa-energiasta/sahkon-ja-lammontuotanto/vesivoima/vesivoima-toimintaperiaate/ (Accessed: 25 January 2019).

Vehviläinen, B., Huttunen, M. (2001). Hydrological Forecasting and Real Time Monitoring in Finland: The Watershed Simulation and Forecasting System (WSFS). Available at: http://www.vyh.fi/tila/vesi/ennuste/index.html (Accessed: 6 February 2019).

Veijalainen, N., Dubrovin, T., Marttunen, M., Vehviläinen, B. (2010). Climate Change Impacts on Water Resources and Lake Regulation in the Vuoksi Watershed in Finland, Water Resour Manage, Vol. 24, pp. 3437–3459. DOI: 10.1007/s11269-010-9614-z.

Veijalainen, N., Jakkila, J. and Nurmi, T., Vehviläinen, B., Marttunen, M., Aaltonen, J. (2012). Suomen vesivarat ja ilmastonmuutos - vaikutukset ja muutoksiin sopeutuminen: WaterAdapt -projektin loppuraportti. Available at: http://www.ymparisto.fi/download.asp?contentid=137197&lan=fi (Accessed 08 January 2019)

Vilkko, M. (1999). New Approach to Short-term Planning of Hydro-thermal Power Production. TTKK.

Wangensteen, I. (2006). Power Markets - TET4185. Available at: http://www.elkraft.ntnu.no/elkraft3/fag/TET4185_Kompendium_06.pdf (Accessed: 18 February 2019).

A. APPENDIX: DISTRIBUTION OF THE FORECAST ERROR

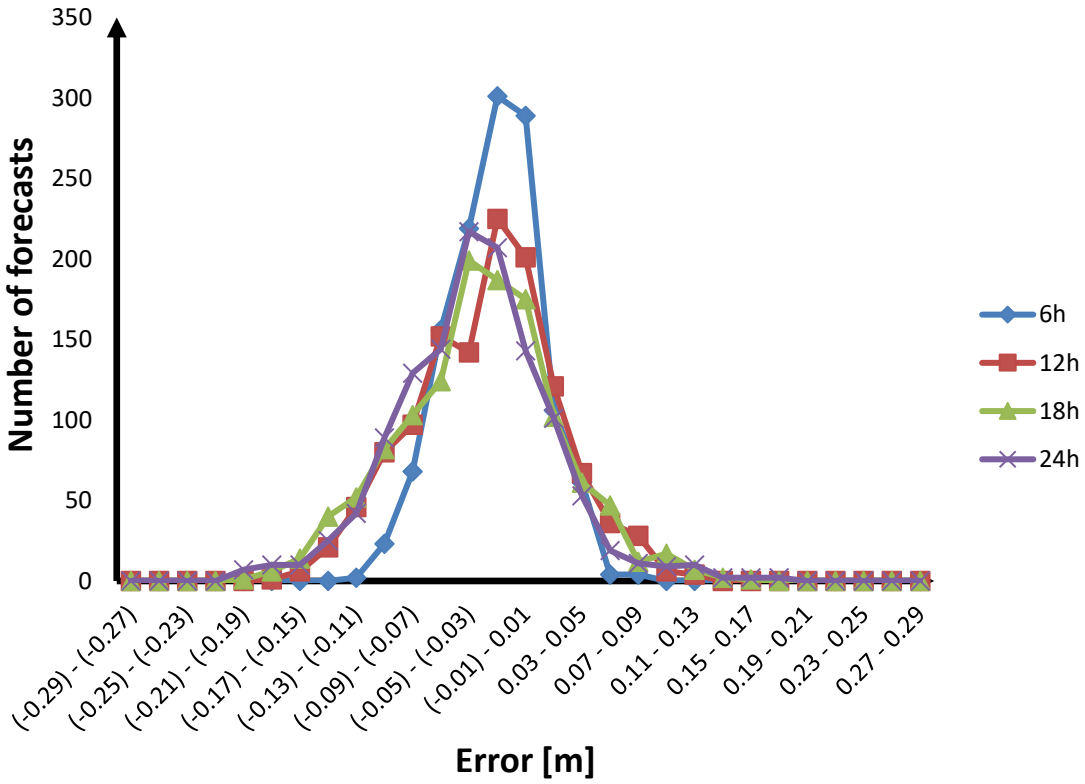

Figure A.1. *The error distribution of L1. The shape of the distribution resembles normal distribution.*

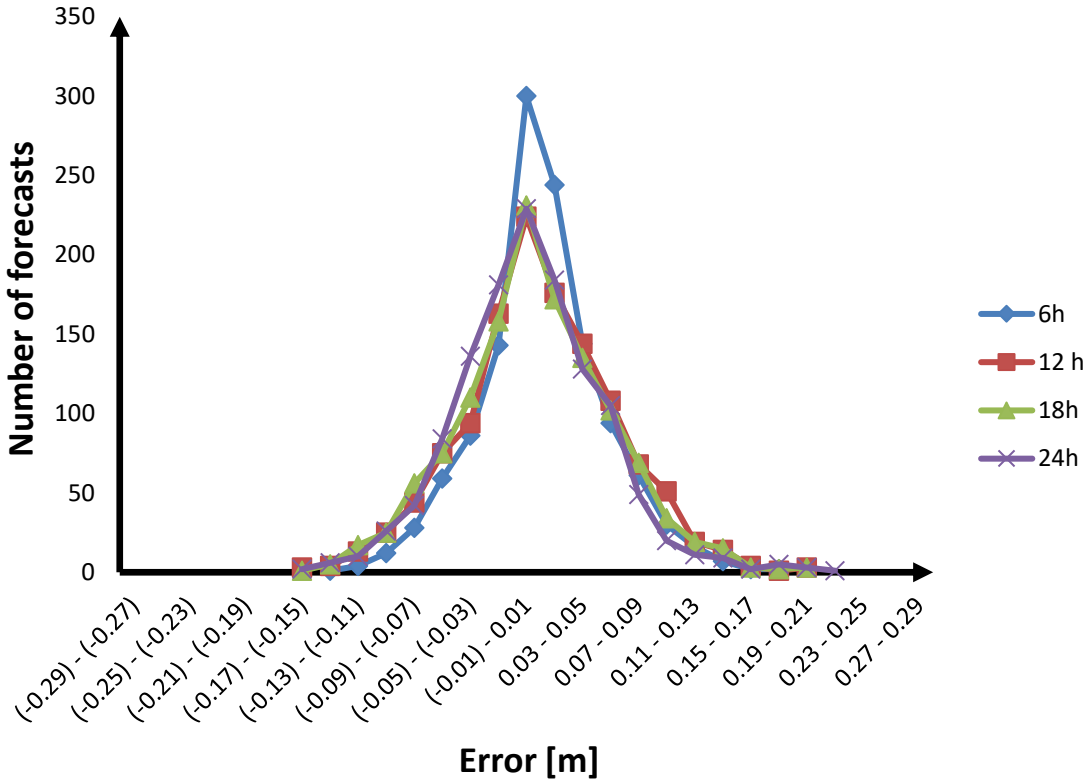

Figure A.2. *The error distribution of L3. The shape of the distribution resembles normal distribution.*

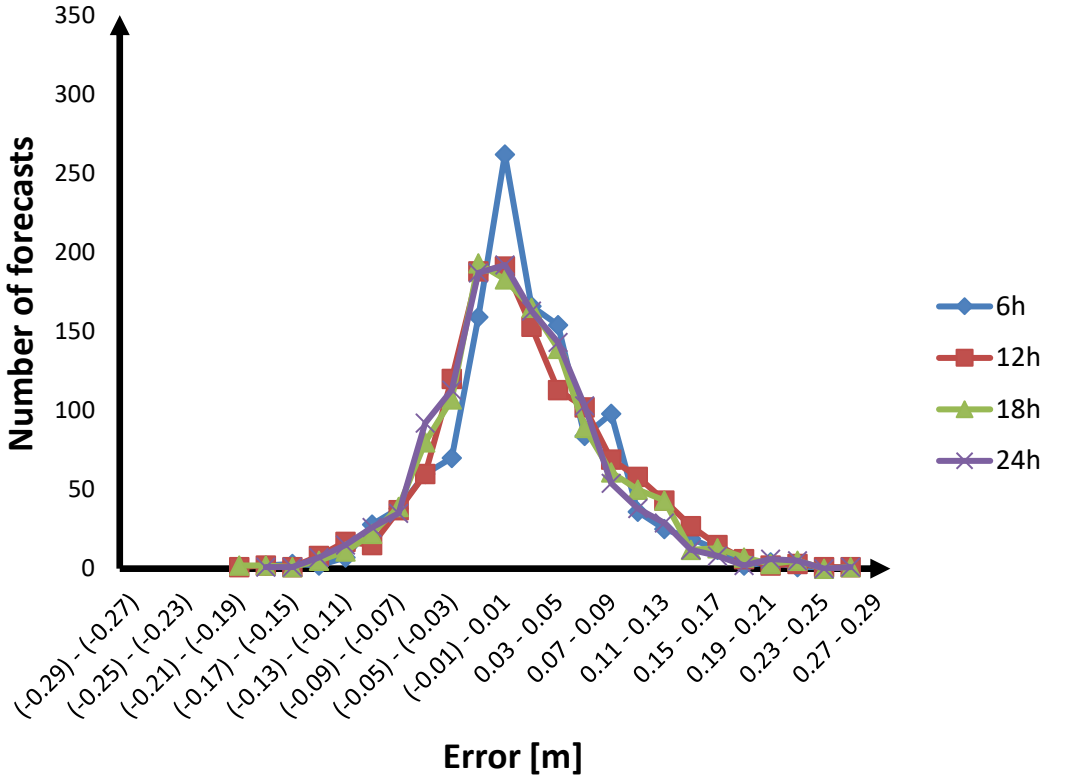

Figure A.3. *The error distribution of L4. The shape of the distribution resembles normal distribution.*